REPORT DOCUMENTATION PAGE

Form Approved
OMB No. 0704-0188

PLEASE DO NOT RETURN YOUR FORM TO THE ABOVE ORGANIZATION.

1. REPORT DATE *(DD-MM-YYYY)*	2. REPORT TYPE	3. DATES COVERED *(From - To)*
01-12-2012	Final Report	06-01-2008 - 05-31-2011

4. TITLE AND SUBTITLE
MOLECULAR GAS-FILLED HOLLOW OPTICAL FIBER LASERS IN THE NEAR INFRARED

5a. CONTRACT NUMBER
FA9550-08-1-0344

5b. GRANT NUMBER

5c. PROGRAM ELEMENT NUMBER

6. AUTHOR(S)
Brian R. Washburn (PI)
Kristan L. Corwin (co-PI)

5d. PROJECT NUMBER

5e. TASK NUMBER

5f. WORK UNIT NUMBER

7. PERFORMING ORGANIZATION NAME(S) AND ADDRESS(ES)
Kansas State University
Pre-award services, 2 Fairchild Hall
Manhattan, KS 66506

8. PERFORMING ORGANIZATION REPORT NUMBER

9. SPONSORING/MONITORING AGENCY NAME(S) AND ADDRESS(ES)
Air Force Office of Scientific Research
875N. Randolph St. Room 3112
Arlington VA 22204

10. SPONSOR/MONITOR'S ACRONYM(S)
AFOSR

11. SPONSOR/MONITOR'S REPORT NUMBER(S)
AFRL-OSR-VA-TR-2012-0270

12. DISTRIBUTION/AVAILABILITY STATEMENT
Approved for public release

13. SUPPLEMENTARY NOTES

14. ABSTRACT
We have demonstrated of a new class of optically pumped gas lasers inside a hollow-core photonic crystal fibers. Here, a molecular gas is confined to a hollow-core photonic crystal fiber whose transmission spans several octaves to reach the mid-infrared spectral region. The gas is pumped in the near-infrared (~1.5 μm) and the laser produces mid-infrared light (~3 μm) offering a potentially robust, efficient, and compact means of producing step-tunable eye-safe mid-infrared radiation well suited to a multitude of applications. During the course of the grant we have demonstrated for the first time mid-infrared lasing in both an acetylene and hydrogen cyanide filled kagome structured hollow-core photonic crystal fiber. These lasers are the first in a new class of infrared lasers based on the combination of hollow-fiber and optically pumped-gas technologies.

15. SUBJECT TERMS
Gas Lasers, Photonic Crystal Fiber, Photonic Bandgap Fiber, Kagome HC-PCF, Mid-Infrared Lasers

16. SECURITY CLASSIFICATION OF:			17. LIMITATION OF ABSTRACT	18. NUMBER OF PAGES	19a. NAME OF RESPONSIBLE PERSON
a. REPORT	b. ABSTRACT	c. THIS PAGE			Brian R. Washburn
U	U	U	UU	43	19b. TELEPHONE NUMBER *(Include area code)* 785-532-2263 washburn@phys.ksu.edu

Reset

Standard Form 298 (Rev. 8/98)
Prescribed by ANSI Std. Z39.18
Adobe Professional 7.0

Final Report
Grant/Contract Title: (DEPSCOR FY08) MOLECULAR GAS-FILLED HOLLOW OPTICAL FIBER LASERS IN THE NEAR INFRARED
Grant/Contract Number: FA9550-08-1-0344
Brian Washburn, Kansas State University, PI
Kristan Corwin, Kansas State University, co-PI

A. Introduction

This report summarizes the major accomplishment of AFOSR DEPSCoR grant number FA9550-08-1-0344 from June 1, 2008 to May 31, 2011 at Kansas State University (K-State). The goal of the project was to demonstrate a proof-of-principle gas-filled hollow core photonic crystal fiber (HC-PCF). During this grant period we accomplished our goal by demonstrating for the first time mid-IR lasing in both an acetylene ($^{12}C_2H_2$) and hydrogen cyanide ($H^{12}CN$) filled kagome structured HC-PCFs. These lasers are the first in a new class of IR lasers based on the combination of hollow-fiber and optically pumped-gas technologies.

A portion of this work was jointly funded by an Army Research Office STTR grant A08A-021-0152. Precision Photonics Corporation (PPC) is the contractor for this grant, where K-State and the University of New Mexico (UNM) are subcontractors. Furthermore, we collaborate with the University of Bath for the kagome fiber used for this work.

B. Summary of Significant Results

B.1. Demonstration of Mid-IR Lasing in an Acetylene Filled HC-PCF

We demonstrated the first gas-filled hollow fiber laser based on population inversion. The laser

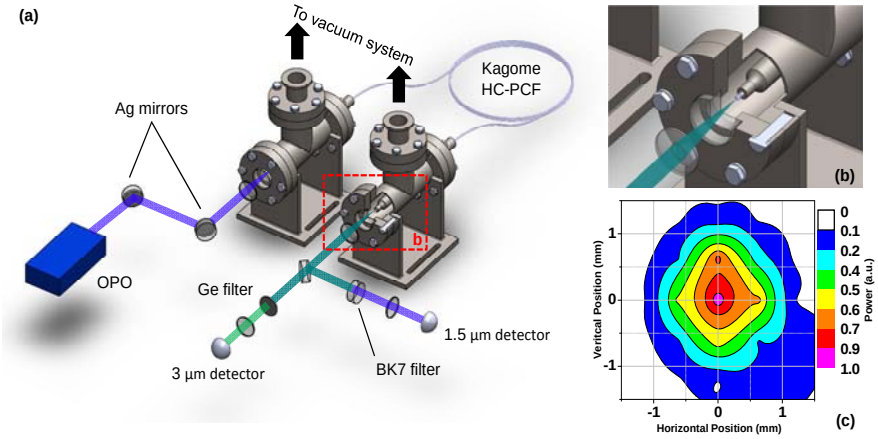

Fig. 1 . Experimental setup and laser beam profile. (a) Pulses from an OPO with a center wavelength of ~ 1.5 μm and 5 ns duration (shown in blue) are coupled into a kagome structured HC-PCF containing low pressure acetylene gas. Pump radiation is absorbed by the gas and laser radiation is detected from ro-vibrational transitions at wavelengths in the mid-IR (shown in green). Laser energy is filtered from pump energy by a polished germanium wafer and detected by a fast, room-temperature HgCdTe photovoltaic detector. (b) Close-up showing a fiber end suspended in a vacuum chamber. (c) Far-field mode profile: power of the collimated 3 μm beam passing through a 750-μm diameter circular aperture as the aperture is scanned transverse to the beam.

setup along with a 3-μm beam profile is shown below. Both ends of the HC-PCF are supported inside vacuum chambers within 1 cm of the windows, allowing light to be coupled through the evacuated fiber. Experiments were performed with 1.65-m and 0.95-m long HC-PCF. BK7 glass

optics couple in pump light at ~ 1.5 μm, while CaF_2 optics couple light out. The laser is pumped with an optical parametric oscillator (OPO) producing pulses roughly 5 ns in duration with a bandwidth of about 3.5 GHz tuned to resonance with the ν1 + ν3 (R7) ro-vibrational transition in C_2H_2 at 1.52106 μm. Polished germanium wafers filter transmitted pump light from mid-IR laser pulses exiting the fiber. An InGaAs photodetector measures pump pulse energy while a fast HgCdTe photodetector observes mid-IR pulses.

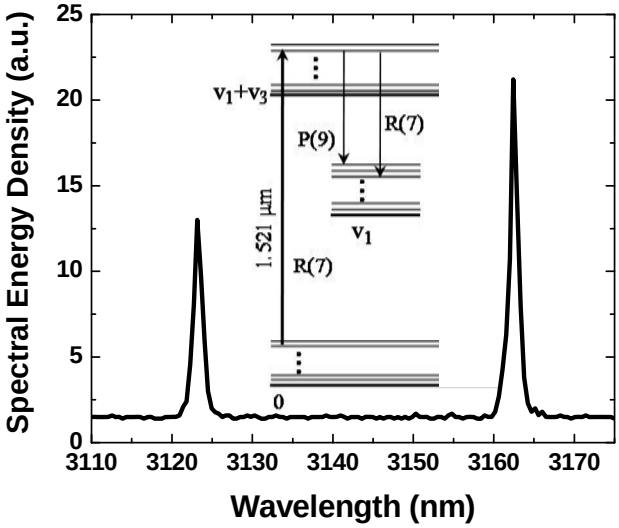

Fig. 2. Spectrum of the acetylene-filled HC-PCF laser. The laser spectrum was taken using a grating spectrometer with ~ 1 nm resolution. The two peaks correspond to transitions from the J = 8, $v_1 + v_3$ pump state to the J = 7 and J = 9, v_1 state, corresponding to wavelengths of 3123.2 nm and 3162.4 nm, respectively. The inset shows pertinent transitions on an energy level diagram.

The initial demonstration of this laser was performed by K-State personnel at the University of New Mexico. A new set-up was constructed at K-State. For this experiment, a 1 ns optical parametric amplifier (OPA) was constructed to pump the laser (see below). As shown in Fig. 3 we demonstrated lasing in an acetylene filled HC-PCF in this system with better efficiency.

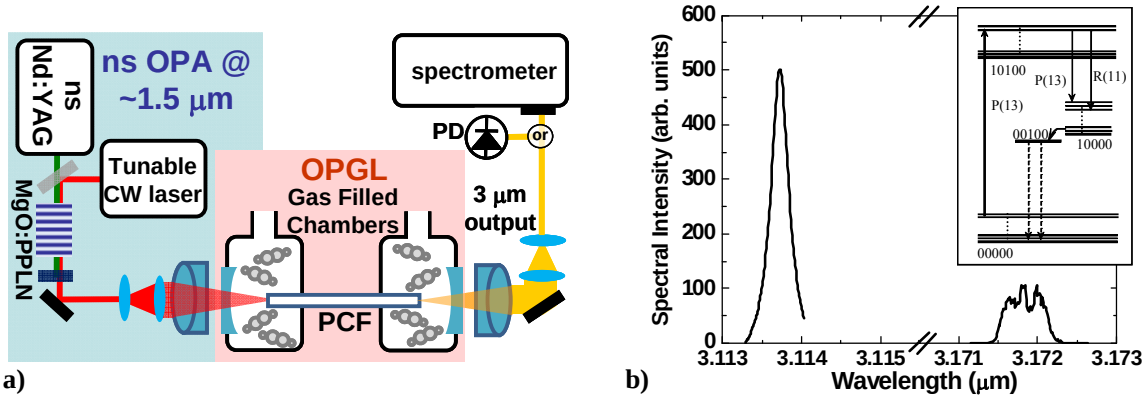

Fig. 3 a) Setup used for both the C_2H_2 and HCN (see below) gas lasers at K-State. b) The spectrum of the C_2H_2 laser pumped at 1.532 μm, where the two peaks correspond to transitions from the J = 12, $v_1 + v_3$ pump state to the J = 11 and J = 12, v_1 state. Inset: C_2H_2 energy transitions.

The measured mid-IR laser pulse energy as a function of absorbed pump pulse energy is shown in Fig. 5 for various acetylene pressures. As the gas pressure is increased from 15 torr, the slope efficiency generally decreases and the laser threshold energy increases. An interesting feature of the low pressure data, is the saturation-type behavior occurring at high absorbed pump pulse energies. This would seem to indicate the onset of an additional process like excited state pump absorption that may remove population from the pumped state at high pump intensities causing additional pump absorption without creating additional mid-IR laser output.

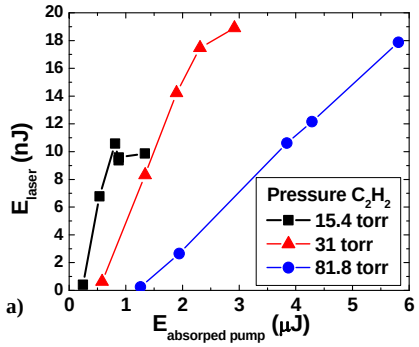

Fig. 4 Plot of measured mid-IR laser pulse energy as a function of absorbed pump pulse energy for a 0.33-m long kagome-structured HC-PCF filled with various pressures of C_2H_2 gas.

B.2. Demonstration of Mid-IR Lasing in a HCN Filled Kagome Fiber

We also demonstrated lasing in a $H^{12}C^{14}N$ filled HC-PCF fiber for the first time. This was demonstrated at K-State using the setup in Fig. 3. The fiber was filled with HCN gas and pumped at 1.541 μm using the OPA exciting to the P(10) state in the $2\nu_1$ band. Lasing at 3.147 and 3.091 μm was measured corresponding to the R(8) and P(10) transitions to the ν_1 band. We are currently investigating the dependence of output power and slope efficiency as a function of HCN gas pressure. This work shows that the HC-PCF laser format can be used for multiple molecular gases to generate mid-IR radiation.

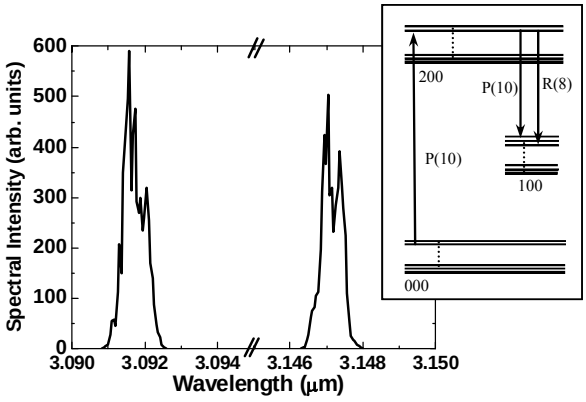

Fig. 5 The spectrum of the HCN laser pumped at 1.541 μm, and the two peaks correspond to transitions from the $J = 9$, $2v_1$ pump state to the $J = 8$ and $J = 10$, v_1 state. The gas pressure was 12.8 and 18.8 torr. Inset: HCN energy transitions.

B.3. Construction of Optical Parametric Amplifier

A nanosecond optical parametric amplifier (OPA) has been designed and constructed at K-State to serve as a high energy pump source for the HCN and C_2H_2 lasers. The OPA amplifies a seed signal at ~1.5 μm using difference frequency generation (DFG) between the signal and an intense nanosecond pump source at 1064 nm. A third idler wavelength will be also produced by DFG. The OPA is illustrated in the figure below. A Nd:YAG laser produces 1 ns, 1 mJ pulses at 1064 nm that are combined with a CW signal from a 1.5 μm laser diode. Both beams are coupled into a 50 mm length periodically poled lithium niobate (PPLN) crystal doped with MgO_2, which increases the nonlinearity. The signal is amplified in the crystal while a new idler beam at 3 μm is produced to conserve energy. Different signal wavelengths ranging from 1.53 to 1.56 μm can be amplified by choosing the appropriate poling period on the crystal and temperature.

The wavelength of the mid-IR idler is related to the Nd:YAG and laser diode wavelength. Thus by tuning the diode one can tune the idler. However, we found that if we do not see the system with the CW laser, an idler is still produced. Since there is no seed laser diode, the idler tunability is not restricted to the tunability of the diode. The idler can be tuned over a wide wavelength range (2.6 to 4 μm) by changing the MgO_2:PPLN poling period and/or temperature. The idler was used to measure the wavelength dependent loss of different HC-PCFs in the mid-IR.

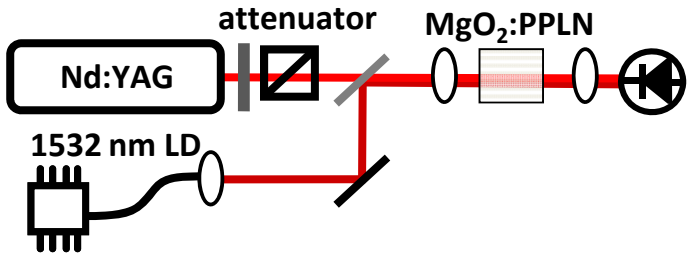

Fig. 6 The set-up for the home-built optical parametric oscillator. The OPO is used to amplify at CW seed laser at ~1.5 μm using DFG pumped by a ns Nd:YAG laser at 1.064 μm. The flexibility of this setup allows us to amplify a range of wavelengths at 1.5 μm, which would be helpful to pump multiple transitions for difference gases. Furthermore, a 3 μm idler is produced.

B.4. HC-PCF Loss Measurements in the Mid-IR (2.6 to 4 μm)

The HC-PCF used for the laser must exhibit low loss at both the pump wavelength (~1.5 μm) and lasing wavelength (~3 μm) in order to obtain a high slope efficiency. The kagome structured HC-PCFs were designed to have low loss (<1 dB/m). However, the loss in the mid-IR for these fibers was unknown. Using the idler from the unseeded OPA described above, we performed fiber cut-back measurements to determine the fibers loss in the mid-IR. A sample loss measurement is shown in Fig. 7. This measurement is extremely time consuming since the idler is tuned by controlling the polling period and/or temperature of the MgO_2:PPLN crystal.

We measured the mid-IR loss in the kagome fibers for the first time. The fiber we used for the initial laser exhibited a loss of 20 dB/m. This measurement has allowed us to find fibers that exhibit low loss for these wavelengths (<10 dB/m).

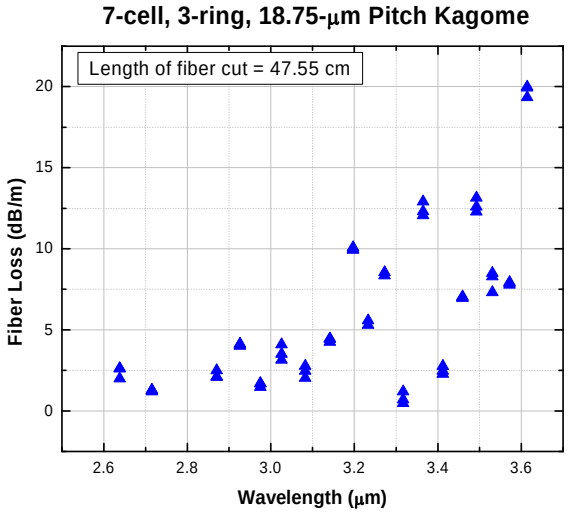

Fig. 7 Wavelength dependent loss of a 7 cell kagome structured HC-PCF. This fiber exhibits less than 1 dB/m loss at 1.5 μm while having a loss less than 5 dB at 3 μm. This is a good candidate fiber for both the C_2H_2 and HCN lasers.

C. Personnel

This work was carried out under the guidance of PI Dr. Brian Washburn and co-PI Dr. Kristan Corwin. Two graduate students, Andrew Jones and Rajesh Kadel, were partially funded by this grant. A portion of this work was jointly funded by an Army Research Office STTR grant A08A-021-0152. We also collaborated with Wolfgang Rudolph at the University of New Mexico, USA and Fetah Benabid at the University of Bath, UK.

D. Publications Produced Under this Grant

Below is a list of all papers and peer reviewed conference submission published under this grant. The papers are enclosed at the end of this report.

D.1. Journal Papers

- A. M. Jones, C. Fourcade-Dutin, C. Mao, B. Baumgart, A. V. V. Nampoothiri, N. Campbell[c], Y. Wang, F. Benabid, W. Rudolph, B. R. Washburn, and K. L. Corwin, "Characterization of mid-infrared emissions from C_2H_2, CO, CO_2, and HCN-filled hollow fiber lasers", to be published in SPIE Journal (2012).
- Andrew M. Jones, A. V. Vasudevan Nampoothiri, Amarin Ratanavis, Tobias Fiedler, Natalie V. Wheeler, François Couny, Rajesh Kadel, Fetah Benabid, Brian R. Washburn, Kristan L. Corwin, and Wolfgang Rudolph, "Mid-infrared gas filled photonic crystal fiber laser based on population inversion," Opt. Express **19**, 2309-2316 (2011) http://www.opticsinfobase.org/oe/abstract.cfm?URI=oe-19-3-2309

D.2. Peer-Reviewed Conference Submissions

- *Invited Presentation*: A. M. Jones, A. V. V. Nampoothiri, A. Ratanavis, T. Fiedler, R. Kadel, W. Hageman, N. Wheeler, F. Couny, F. Benabid, W. Rudolph, K. L. Corwin, and B. R. Washburn, "Mid-IR Fiber Lasers Based on Molecular Gas-filled Hollow-Core Photonic Crystal Fiber" CLEO:2011 - Laser Applications to Photonic Applications, OSA Technical

Digest (CD) (Optical Society of America, 2011) http://www.opticsinfobase.org/abstract.cfm?URI=CLEO: S and I-2011-CThD1

- *Invited Presentation*: W. Rudolph, A.V. Nampoothiri, A. Ratanavis, A. Jones, R. Kadel, B.R. Washburn, K.L. Corwin, N. Wheeler, F. Couny, F. Benabid, "Mid-IR laser emission from a C_2H_2 gas filled hollow core fiber," Transparent Optical Networks (ICTON), 2010 12th International Conference on , Digital Object Identifier: 10.1109/ICTON.2010.5549075 (Tu.B2.4), Page(s): 1-4 (2010) http://ieeexplore.ieee.org/xpls/abs_all.jsp?arnumber=5549075
- V. Nampoothiri, A.M. Jones, A.M.; A. Ratanavis, N. Campbell, R. Kadel, N. Wheeler, F.Couny, F. Benabid, B.R. Washburn, K.L. Corwin, W. Rudolph, "Optically Pumped C_2H_2 and HCN Lasers with Conventional Cavities and Based on Hollow Core Photonic Crystal Fibers", INTERNATIONAL SYMPOSIUM ON HIGH POWER LASER ABLATION 2010, AIP Conference Proceedings, v 1278, p 749-57, (2010) http://link.aip.org/link/?APCPCS/1278/749/1
- Jones, A.M., Nampoothiri, A.V.V.; Ratanavis, A.; Kadel, R.; Wheeler, N.V.; Couny, F.; Benabid, F.; Rudolph, W.; Washburn, B.R.; Corwin, K.L. , "C_2H_2 Gas Laser Inside Hollow-Core Photonic Crystal Fiber Based on Population Inversion", Source: 2010 Conference on Lasers and Electro-Optics (CLEO), p 2 pp., (2010) http://ieeexplore.ieee.org/stamp/stamp.jsp?tp=&arnumber=5500152
- *Post-Deadline Paper*: A.V.V. Nampoothiri, A. Jones , A. Ratanavis, K. Corwin, B.R. Washburn, W. Rudolph, "Laser emission from a gas (acetylene) filled hollow fiber", Photonics West, Jan. 2010, San Francisco, CA

E. Conclusion and Future Work

As demonstrated above we have made substantial progress toward the development of mid-IR fiber gas lasers. We are continuing this work investigating different HC-PCFs and different molecular gases. We are also pursuing high quantum efficiency lasing in the near-IR by pumping and lasing on nearby ro-vibrational levels.

Characterization of mid-infrared emissions from C_2H_2, CO, CO_2, and HCN-filled hollow fiber lasers

A. M. Jones[a], C. Fourcade-Dutin[b], C. Mao[c], B. Baumgart[c], A. V. V. Nampoothiri[c], N. Campbell[c], Y. Wang[b], F. Benabid[b,d], W. Rudolph[c], B. R. Washburn[a], and K. L. Corwin*[a]
[a]Dept. of Physics, Kansas State Univ., Manhattan, KS USA 66506;
[b]Centre for Photonics and Photonic Materials, Dept. of Physics, Univ. of Bath, Claverton Down, Bath BA2 7AY, United Kingdom;
[c]Dept. of Physics and Astronomy, Univ. of New Mexico, Albuquerque, NM USA 87131;
[d]Xlim Research Institute, CNRS UMR 6172, Université de Limoges, 87060 Limoges, France

ABSTRACT

We have now demonstrated and characterized gas-filled hollow-core fiber lasers based on population inversion from acetylene ($^{12}C_2H_2$) and HCN gas contained within the core of a kagome-structured hollow-core photonic crystal fiber. The gases are optically pumped via first order rotational-vibrational overtones near 1.5 μm using 1-ns pulses from an optical parametric amplifier. Transitions from the pumped overtone modes to fundamental C-H stretching modes in both molecules create narrow-band laser emissions near 3 μm. High gain resulting from tight confinement of the pump and laser light together with the active gas permits us to operate these lasers in a single pass configuration, without the use of any external resonator structure. A delay between the emitted laser pulse and the incident pump pulse has been observed and is shown to vary with pump pulse energy and gas pressure. Furthermore, we have demonstrated lasing beyond 4 μm from CO and CO_2 using silver-coated glass capillaries, since fused silica based fibers do not transmit in this spectral region and chalcogenide fibers are not yet readily available. Studies of the laser pulse energy as functions of the pump pulse energy and gas pressure were performed. Efficiencies reaching ~ 20% are observed for both acetylene and CO_2.

Keywords: Optically pumped gas laser, molecular gas, mid-infrared, photonic crystal fiber, kagome fiber, metal-coated waveguide, capillary

A. INTRODUCTION

Laser sources operating at mid-infrared (mid-IR) wavelengths have become increasingly popular. This retina-safe region of the spectrum contains several windows of high atmospheric transmission, well suited to a variety of applications such as remote sensing, free space communications, and range finding. Additionally, the mid-IR spectral region coincides with fundamental rotational-vibrational transitions in many molecules including hazardous pollutants and greenhouse gases like NO and NO_2, CO and CO_2, N_2O, and CH_4. Furthermore, the transition strengths of these fundamental transitions are generally orders of magnitude stronger than corresponding overtone transitions that lie at shorter wavelengths within the near infrared or visible regions of the spectrum, making mid-IR sources a natural choice for applications involving trace gas detection and molecular fingerprinting such as breath analysis and stand-off explosives detection.

Optically pumped gas lasers in waveguides offer many advantages over traditional gas laser geometries and may provide a simple, compact, and robust means of generating mid-IR light. Waveguides can function as unfolded cavities that permit long interaction lengths between the pump and generated laser light and the gas medium within small mode areas, on the order of 100 μm^2. Kagome-structured hollow-core photonic crystal fiber (HC-PCF) permits ultra-broad, multi-octave spanning spectral guidance [1], and can be spliced to solid-core fibers, creating compact, robust sealed gas cells [2]. However, HC-PCF made from fused silica has not yet been demonstrated to guide with reasonable loss beyond ~ 3.6 μm. At these longer wavelengths, metal coated glass capillaries offer a solution, with calculated losses below 10 dB/m for wavelengths beyond 6.0 μm.

*corwin@phys.ksu.edu; phone 1 785 532-1645; fax 1 785 532-6806

B. C_2H_2 and HCN-filled HC-PCF lasers

B.1. Hollow-core photonic crystal fibers

There are generally two classes of HC-PCFs: photonic band gap fibers (PBGF) and kagome-structured fibers. As the name suggests, PBGF employs a band gap to guide light in its hollow core. Essentially, the cladding structure of the PBGF creates wavelength regions where no photonic states are permitted to exist within the cladding. Therefore, light within this wavelength region is confined to the cladding defect, *i.e.* the hollow core, where it can propagate with low loss [3]. Unfortunately, the spectral width of the band gap region is limited to less than the octave we require for our lasers [4].

Kagome-structure HC-PCFs on the other hand have been demonstrated to guide multiple octaves with low loss [1]. However, because these fibers are made from fused silica and are typically optimized for performance at visible and near infrared wavelengths, most existing kagome fibers exhibit relatively large loss at mid-IR wavelengths, *e.g.* ~ 20 dB/m at 3.16 μm. Using finite element analysis software like JCMwave to optimize the fiber loss profile, kagome fibers exhibiting low loss regions in both the near and mid-IR can be designed which should be suitable for use in gas-filled fiber lasers. Calculating the fiber loss for these microstructured fibers is computationally intensive and time consuming. We instead have gone with a coarser, much quicker approach where we use empirical rules to scale existing designs to create fibers with the desired loss profiles. We then test these fibers of varying pitch and strut thicknesses via cut-back measurements to map out the fiber loss characteristics. A white light source and a commercial optical spectrum analyzer are used for loss measurements in the visible and near infrared, while the tunable mid-IR idler from an optical parametric amplifier (OPA) and a HgCdTe detector are used to measure the mid-IR fiber loss. The loss profile of the particular kagome-structured HC-PCF used in the mid-IR laser work discussed here, is shown in Fig. 1. The fiber's kagome cladding structure can be seen from the scanning electron microscope (SEM) image of the fiber cross section shown in the Fig. 1 inset. The fiber loss at 1.5 μm, in the region of the pump wavelengths, is seen to be ~ 0.1 dB/m, while the loss at 3.14 μm, near the laser wavelengths, is just below 5 dB/m. This represents a more than twenty-fold reduction in fiber loss from the previous fiber used in the laser setup [5].

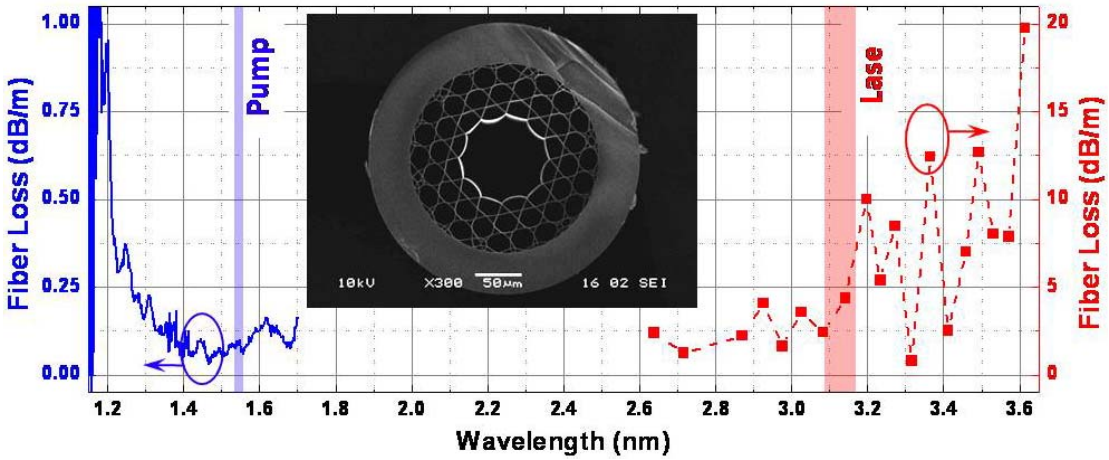

Figure 1. Measured loss spectrum of the kagome-structured HC-PCF used in the laser. The pump wavelengths are contained within the blue line near 1.5 μm, and the mid-IR laser wavelengths are contained within the red line just beyond 3 μm. Inset: SEM image of the fiber end. The fiber is seen to have a pitch of 18.75 μm and a core diameter of 85 – 94 μm.

B.2. C_2H_2 and HCN-filled HC-PCF laser setup

A schematic of the C_2H_2 and HCN-filled HC-PCF laser setup is shown in Fig. 2. The setup centers around a 45 cm or 1.46 m length of kagome-structured HC-PCF. The fiber ends are supported in vacuum chambers allowing the hollow core of the fiber to be filled with various pressures of either C_2H_2 or HCN gas. Windows on each vacuum chamber allow the pump light to be coupled into the fiber and the generated mid-IR laser light along with any unabsorbed pump light to be coupled out. The molecules contained within the hollow fiber are pumped via narrow-band, ~ 1-ns duration pulses from a homebuilt OPA. Inside the OPA, pump pulses from a Nd:YAG laser are mixed with continuous wave (CW) light from a tunable fiber or extended cavity diode laser inside of a MgO:PPLN crystal

to produce the ~ 1-ns duration, microjoule-scale pulse energies used to excite the molecular gases. The center wavelength of the pulses from the OPA tune with the wavelength of the CW seed laser, allowing the pump pulses to be tuned to precise resonance with any particular rotational-vibrational (ro-vibrational) transition of the acetylene or HCN molecules in the 1.5-μm wavelength region. Once coupled out of the fiber, the generated mid-IR laser pulses are filtered from the transmitted pump light using a 2-mm thick, antireflection-coated germanium filter. The mid-IR laser pulses are then either sent to a fast HgCdTe photodetector for energy and timing measurements or to a single-pass grating monochrometer for spectral measurements. Prior to any filtering, a small portion of the main beam coupled out of the fiber end is picked-off via a CaF_2 window and coupled into a single mode fiber. By optimizing the freespace-to-fiber coupling for the pump light and because of the relatively long fiber length and the short attenuation length of fused silica beyond 3 μm, the mid-IR laser light is filtered from the pump light, allowing just the transmitted pump pulses to be detected by a fiber coupled, 25-GHz InGaAs photodetector.

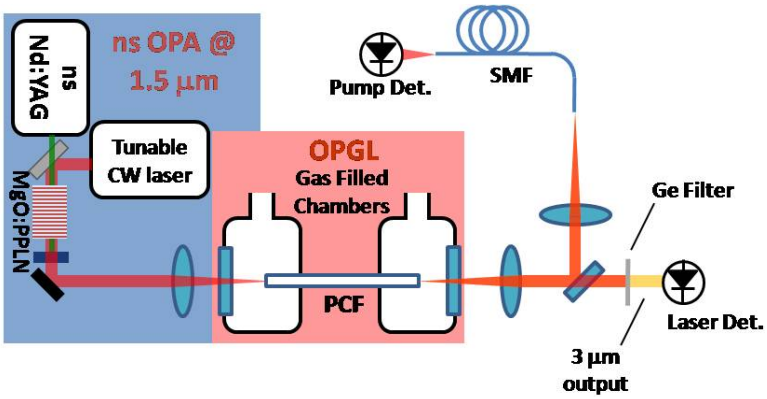

Figure 2. Gas-filled HC-PCF laser setup. C_2H_2 or HCN gas is contained inside the HC-PCF. Pump pulses from an OPA are coupled into the fiber through one end while the generated mid-IR light and any unabsorbed pump light are coupled out of the opposite end of the fiber. Mid-IR light passes through a 2-mm thick germanium filter and is focused onto a HgCdTe detector. A fraction of the unabsorbed pump light is picked off from the main beam and then sent to a fiber coupled, 25-GHz InGaAs detector.

B.3. C_2H_2 laser results and discussion

Acetylene gas inside of a 1.46-m long piece of the 18.75-μm pitch kagome fiber is pumped at a wavelength of 1532.8 nm corresponding to the P(13) overtone transition between the vibrational ground state and the $\nu_1 + \nu_3$ vibration state, *i.e.* j = 13, vibrational ground state → j = 12, $\nu_1 + \nu_3$ state. For clarity, the normal modes of vibration for the acetylene molecule are shown in Fig. 3 [6]. The ν_1 vibrational mode is seen to correspond to the symmetric C–H stretch, while the ν_3 vibrational mode corresponds to the anti-symmetric stretch. The pump pulse excites a fraction of the population from the j = 13 ground state to the j = 12 excited state. This very quickly creates a population inversion between the pumped state and both the dipole allowed j = 11 and j = 13, ν_1 states, since the thermal population of the ν_1 states at room temperature is negligible. Since there is no dipole allowed transition from the ν_1 states directly to the ground vibrational state, we expect that once the intensity of stimulated emission is sufficient to equalize the populations between the pumped state and the ν_1 states, the laser action will stop and no additional transitions will be observed.

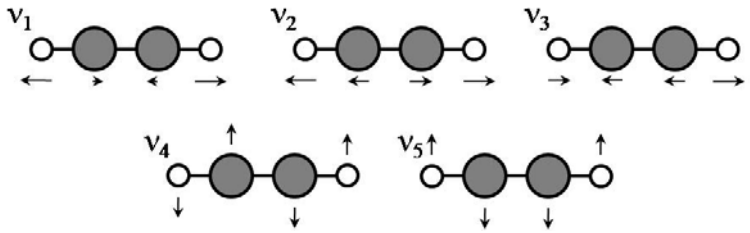

Figure 3. The five non-degenerate normal modes of C_2H_2. The small white-filled circles represent hydrogen atoms while the larger, gray-filled circles represent carbon atoms. The relative motions of the hydrogen and carbon atoms comprising the molecules are indicated by the black arrows (not to scale) above or below each atom. The label $\nu_1 - \nu_5$, corresponding to each normal mode, is shown at the upper left of the molecules.

The measured spectra of the mid-IR laser pulses taken at various acetylene pressures are shown in Fig. 4 along with an energy level diagram shown in the inset, illustrating the relevant transitions. The measured peak wavelengths match well with the expected R(11), *i.e.* j = 12, $\nu_1 + \nu_3$ state → j = 11, ν_1 state, and P(13) transition wavelengths of 3114.6 and 3172.4 nm respectively. The total energy of the laser pulse which is proportional to the area under the spectral curves is seen to reach a maximum at a pressure of 20 torr. The R-branch transition is seen to always be favored by a factor of ~ 2 – 5, and the relative contribution to the laser energy from the two transitions involved is not seen to be grossly pressure dependent.

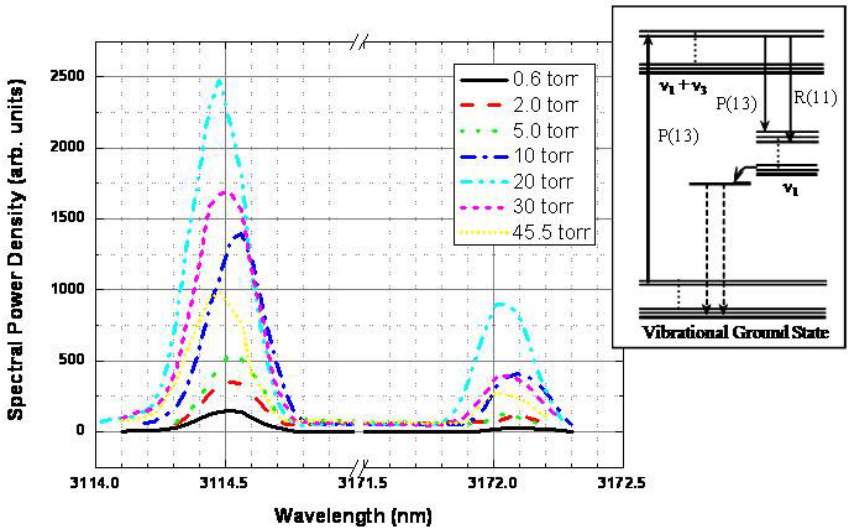

Figure 4. Measured spectra of the mid-IR laser pulse taken at different acetylene pressures. Inset: An energy level diagram showing the relevant ro-vibrational transitions.

The measured mid-IR laser pulse energy as a function of absorbed pump pulse energy is shown in Fig. 5 for various acetylene pressures. The laser efficiency, defined as the ratio of the laser pulse energy to the absorbed pump pulse energy, is seen to reach a maximum of more than 20% at 2.00 torr. As the gas pressure is increased from 2.0 torr, the slope efficiency generally decreases and the laser threshold energy increases (except at 20 torr in this preliminary data). An interesting feature of the low pressure data, 5.0 torr and below, is the saturation-type behavior occurring at high absorbed pump pulse energies. This would seem to indicate the onset of an additional process like excited state pump absorption that may remove population from the pumped state at high pump intensities causing additional pump absorption without creating additional mid-IR laser output.

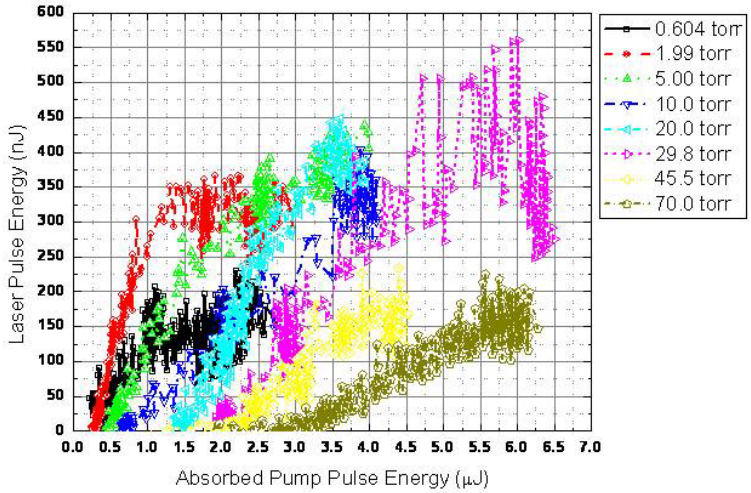

Figure 5. Plot of measured mid-IR laser pulse energy as a function of absorbed pump pulse energy for a 1.46-m long kagome-structured HC-PCF filled with various pressures of C_2H_2 gas.

The observed peak-to-peak delay between the generated mid-IR laser pulse and the absorption-free transmitted pump pulse as a function of the absorbed pump pulse energy is shown in Fig. 6 for various acetylene pressures. The delays are seen to range from near zero to beyond 30 ns. Generally, for high absorbed pulse energies the delay seems to be quite small, indicating that the laser pulse power continues to grow until just after the peak of the pump pulse. For lower absorbed pump pulse energies, the laser power peak arrives later relative to the absorption-free pump pulse, likely indicating that for low energy pump pulses more time is needed for the molecules to absorb enough energy to produce the maximum population inversion and thus the maximum laser power. Striation in the delays for the lowest pressure data arises from the fact that multiple peaks can be seen in the temporal profile of the laser pulse, and the relative height of these peaks changes from pulse to pulse.

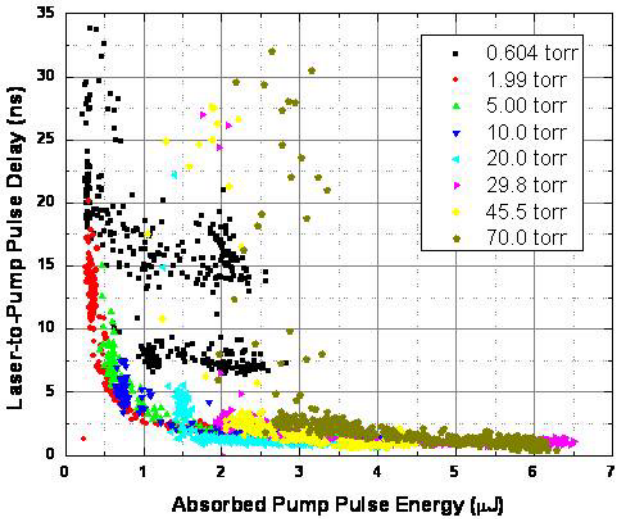

Figure 6. The observed peak-to-peak delay between the generated mid-IR laser pulse and the absorption-free transmitted pump pulse as a function of the absorbed pump pulse energy at various acetylene pressures. The scatter in the delays at relatively low absorbed pump energies and high pressures is likely noise from working near threshold.

B.4. HCN laser results and discussion

HCN gas inside of a 45-cm length long piece of the 18.75-μm pitch kagome fiber is pumped at a wavelength of 1541.3 nm corresponding to the P(10) overtone transition between the vibrational ground state and the $2\nu_3$ vibration state. For clarity the normal modes of vibration for the HCN molecule are shown in Fig. 7 [6]. The ν_3 vibrational mode is seen to correspond to the asymmetric C–H stretch. The pump pulse excites population from the j = 10 ground state to the j = 9 excited state, creating a population inversion between the pumped state and both the dipole allowed j = 8 and j = 10, ν_3 states. Like acetylene, HCN is linear, but unlike acetylene none of the normal modes of HCN are symmetric. This lack of symmetry may allow a more complete relaxation of the excited populations permitting more efficient lasing. However, we do not expect to see contributions to the laser pulse energy from transitions between the ν_3 states and the vibrational ground states. This is because even though these transitions are allowed, the thermal populations in the j = 7, 9, and 11 vibrational ground states at room temperature should be on the order of the total population initially in the j = 10 pump state. Thus no inversion should exist.

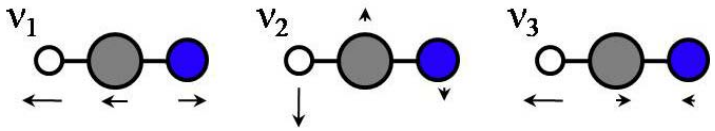

Figure 7. The three normal modes of HCN. The small white-filled circles represent hydrogen atoms; the larger, gray-filled circles represent carbon atoms, and the medium sized blue-filled circles represent nitrogen atoms. The relative motions of the atoms comprising the HCN molecule are indicated by the black arrows (not to scale) above and below each atom. The label ν_1 – ν_3, corresponding to each normal mode, is shown at the upper left of the molecules.

The measured spectrum of the mid-IR laser pulse from the HCN laser is shown in Fig. 8, while the inset shows an energy level diagram with the relevant transitions. In contrast to the acetylene laser, the HCN laser spectrum indicates that the longer wavelength P-branch transition is favored.

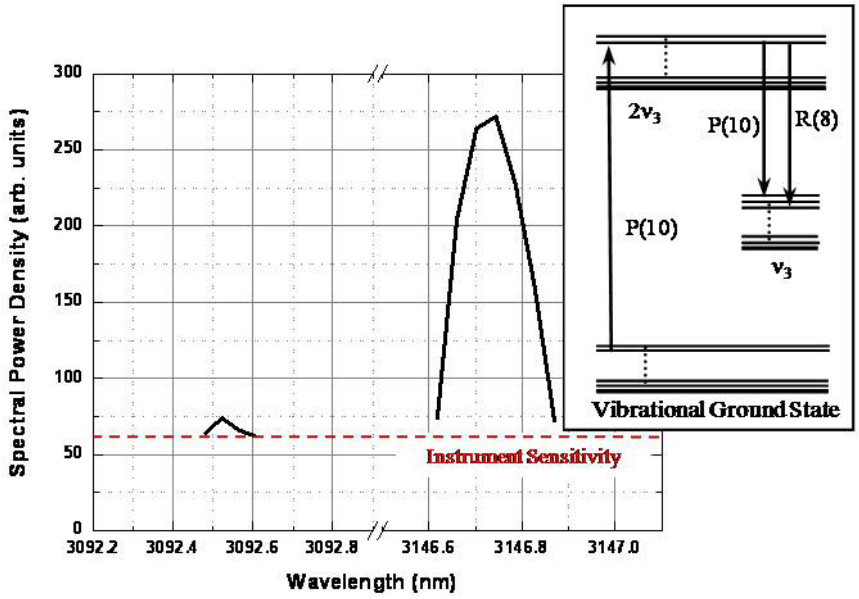

Figure 8. Spectrum of the mid-IR laser pulses created in a 45-cm long kagome-structured HC-PCF filled with 11.6 torr of HCN gas. The horizontal dashed red line indicates the limitation imposed by the instrument's sensitivity. Inset: An energy level diagram showing the relevant ro-vibrational transitions.

Figure 9 shows the maximum observed laser pulse energy as a function of absorbed pump pulse energy for various pressures of HCN gas contained within the 45-cm long hollow fiber. The maximum laser pulse energy is ~ 56 nJ and occurs at 8.0 torr. This is about a factor of 10 lower than the maximum laser pulse energy produced by the acetylene laser.

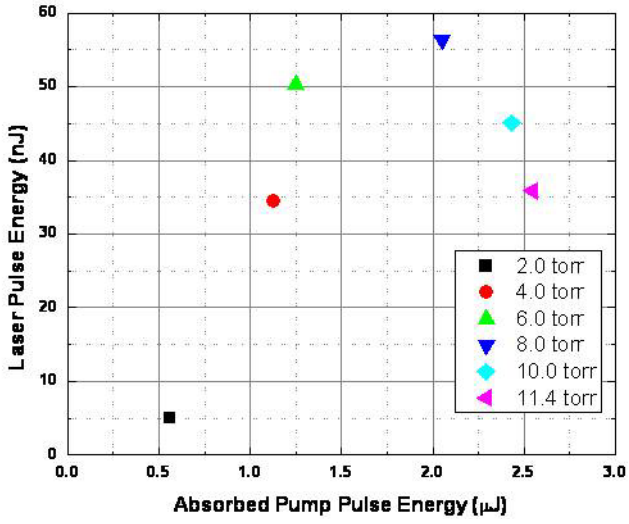

Figure 9. Maximum laser pulse energy as a function of absorbed pump pulse energy for various pressures of HCN gas contained within a 45-cm long kagome-structured HC-PCF.

C. CO and CO_2-filled silver-coated capillary lasers

C.1. Metal-coated capillaries

While successful mid-IR guidance from HC-PCFs has been demonstrated [7], development of both fused silica and chalcogenide fibers exhibiting low loss guidance reaching beyond 3.6 um remains a challenge. In the mean time we have begun exploring gas-filled fiber lasers operating in this spectral region using silver-coated capillaries to confine the light and gas together. These coated capillaries provide us a test bed for longer wavelength gas-filled fiber lasers while suitable fibers are being developed.

Under optimal coupling, the free-space TEM00 mode couples to the EH11 waveguide mode with ~ 98% efficiency [8]. The waveguide power loss for the dominant EH11 mode is given by the equation [9],

$$\alpha = \frac{1}{2}\left(\frac{2.405}{\pi}\right)^2 \frac{\lambda^2}{a^3}\,\mathrm{Re}\left(\frac{1}{2}\frac{n^2+1}{\sqrt{n^2-1}}\right) \qquad (1)$$

where λ is the wavelength, *a* is the radius of the waveguide, and *n* is the complex refractive index. Using Eq. 1, the theoretical loss for a 500-μm diameter silver-coated waveguide is shown in Fig. 10, along with the calculated loss for a 40-μm diameter kagome fiber [5]. The spectral region shown includes the pump and laser wavelengths for the CO and CO_2–filled waveguide lasers which are indicated by the vertical dashed lines. The loss of the kagome fiber is seen to increase very rapidly to beyond 1000 dB/m at wavelengths approaching 3.5 μm. Conversely, the loss of the silver-coated waveguide is just below 1 dB/m in the 4.5-μm region, near the CO and CO_2 laser wavelengths, making this 500-μm diameter silver-coated waveguide a suitable fiber to explore lasing at these wavelengths. From Fig. 10 the loss for the pump wavelengths is estimated to be ~ 0.04 dB/m, while the estimated loss for the laser wavelengths is ~ 0.9 dB/m.

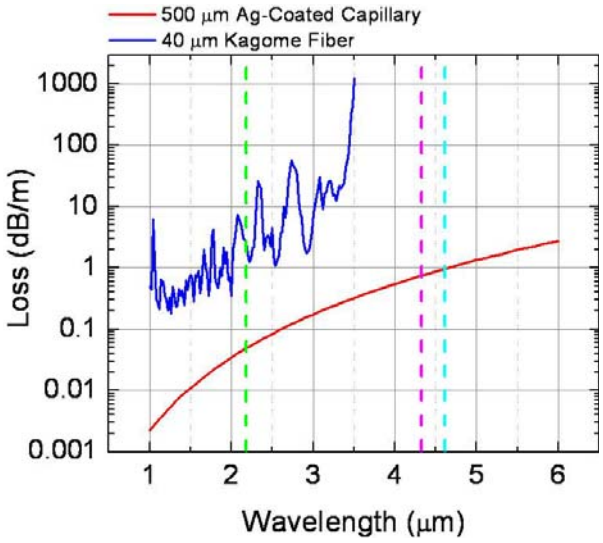

Figure 10. Theoretical loss for the 500-μm diameter, silver-coated capillary (red curve) and for a kagome-structured HC-PCF (blue curve) with a core diameter of 40 μm. The wavelength region of the pump is indicated by the vertical green dashed line while the CO and CO_2 laser wavelength regions are indicated by the vertical cyan and magenta dashed lines respectively.

C.2. CO and CO_2-filled waveguide laser setup

The basic setup for the waveguide laser is shown in Fig. 11. Just as in the HC-PCF laser setup, both ends of a ~ 1.5-m long, inner wall silver-coated capillary with an inner diameter of 500 μm are terminated in vacuum chambers to facilitate filling the fibers with various pressures of either CO or CO_2. Coupling through the waveguide, detector positioning, and general optical alignment is optimized using the pump beam with the waveguide evacuated. The gases are optically pumped using pulses from an optical parametric oscillator (OPO) tuned to resonance with particular ro-vibrational overtones in the molecules. The pump pulses are 5 ns in duration with energies up to ~ 1 mJ at a wavelength of ~ 2 μm with a bandwidth of ~ 3.5 GHz. Pump pulses are coupled into one end of the waveguide while the generated mid-IR laser pulses along with the unabsorbed pump pulses are coupled out the

opposite end, filtered, and detected. For spectral measurements the mid-IR laser output was redirected into a near infrared monochromator. In the case of both CO and CO_2, the gain was high enough to generate lasing in a single pass, avoiding the need for an external resonator.

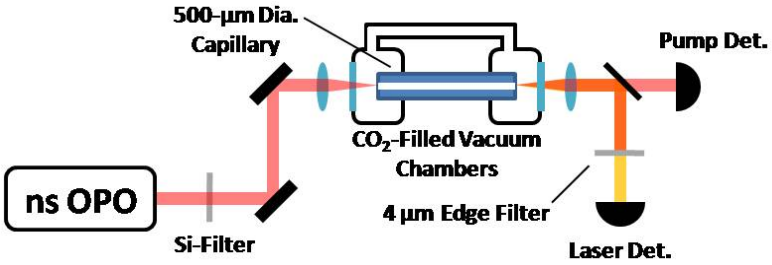

Figure 11. Gas-filled silver-coated capillary laser setup. The gases are pumped using 5-ns duration pulses from an OPO tuned to resonance with ro-virational overtones at ~2 μm coupled into one end of the waveguide. The generated mid-IR laser pulses as well as the unabsorbed pump pulses are coupled out the opposite end of the fiber, filtered, and detected.

C.3. CO laser results and discussion

The CO laser is pumped at a wavelength of 2331.9 nm corresponding to the R(7) overtone transition between the v = 0 vibrational ground state and the v = 2 vibration state. The pump pulse excites population from the j = 7 ground state to the j = 8 excited state. Figure 12 shows the spectrum of the mid-IR laser pulses generated from the CO-filled (50 torr) waveguide laser together with an energy level diagram showing relevant transitions. From the spectroscopic constants, the peaks in the measured laser spectrum correspond to the R(7) and P(6), v = 2 → 1 transitions.

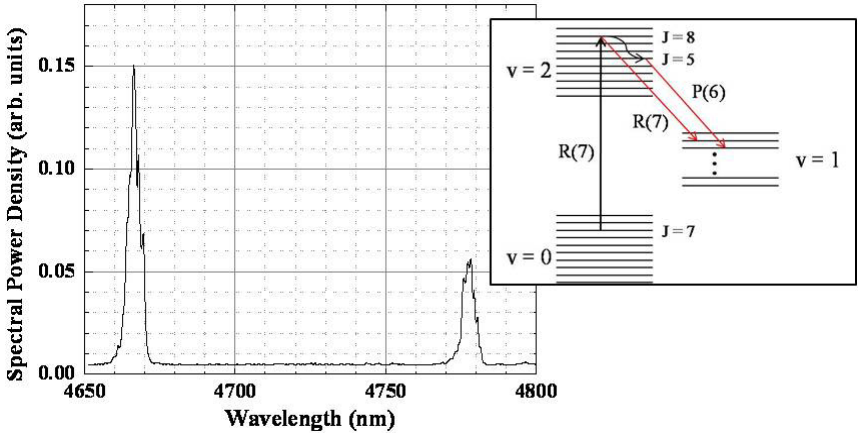

Figure 12. Spectrum of the mid-IR output from the CO-filled waveguide laser taken at 50 torr. Inset: Energy level diagram showing the pump transition along with the assigned laser transitions

C.4. CO_2 laser results and discussion

The CO_2 laser is pumped at a wavelength of 2002.5 nm corresponding to the R(22) overtone transition between the vibrational ground state and the $2\nu_1 + \nu_3$ vibration state. For clarity the normal modes of vibration for the CO_2 molecule are shown in Fig. 13 [6]. The ν_1 vibrational mode is seen to correspond to the symmetric C–O stretch, while the ν_3 vibrational mode corresponds to the anti-symmetric stretch. The pump pulse excites a fraction of the population from the j = 22 ground state to the j = 23 excited state which creates the population inversion leading to the laser emissions.

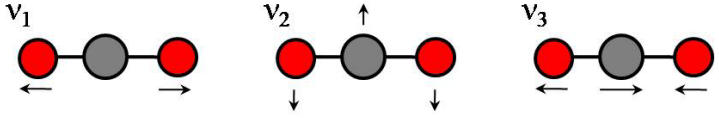

Figure 13. The 3 normal modes of CO_2. The red-filled circles represent oxygen atoms while the gray-filled circles represent carbon atoms. The relative motions of the atoms comprising the CO_2 molecule are indicated

by the black arrows (not to scale) above and below each atom. The label $\nu_1 - \nu_3$, corresponding to each normal mode, is shown at the upper left of the molecules.

As can be seen from Fig. 14, two lasing lines are observed in the 4.3-μm region. The inset in Fig. 14 shows a schematic of the CO_2 energy level diagram with our interpretation of the observed lasing lines. From the spectroscopic constants of the molecule, our preliminary assessment is that the peak near 4.30 μm corresponds to the expected R(22) transition between the terminal pump state and the lower lying j = 22, $2\nu_1$ ro-vibrational state, while the peak near 4.37 μm likely corresponds to the transition from j = 17, $2\nu_1 + \nu_3 \rightarrow$ j = 18, $2\nu_1$; the j = 17 in the upper state being populated during relaxation from the initially populated j = 23 pump level. It is also possible that the 4.37 μm spectral component arises from transitions between the Fermi-resonant $\nu_1 + \nu_3$, $2\nu_2 + \nu_3$ states and the ν_1, $2\nu_2$ states or from transitions from the $\nu_2 + \nu_3$ state to the ν_2 state.

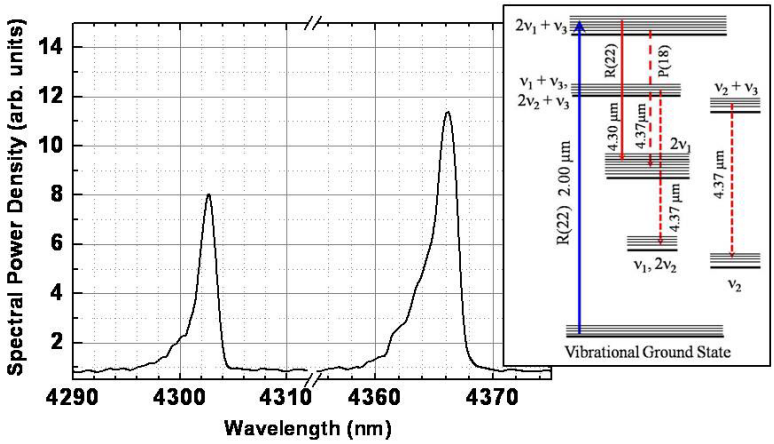

Figure 14. Measured spectrum of the mid-IR laser pulse from the CO_2-filled waveguide laser taken at ~ 5 torr. Inset: An energy level diagram showing both the expected (solid red arrows) and the possible, additional (dashed red arrows) ro-vibrational transitions contributing to the laser pulse.

Figure 15(a) shows the mid-IR laser pulse energy as a function of absorbed pump pulse energy for the waveguide CO_2 laser. For this measurement, the gas pressure was kept at the optimum value of ~ 100 torr. A maximum laser pulse energy of ~ 100 μJ corresponding to a laser efficiency of ~ 20% is observed from the waveguide laser. The measured lasing threshold occurs at ~ 40 μJ of absorbed pump pulse energy.

Figure 15(b) shows the laser pulse energy as a function of gas pressure for the two spectral components comprising the laser pulse. The optimum pressure for the 4.37 μm component (unfilled circles) is ~ 100 torr, while the optimum pressure for the 4.30 μm component (red-filled circles) is ~ 15 torr. The observed pressure dependence can be understood in terms of interplay between pressure broadening, pressure dependent number densities, and collisional relaxation rates which reduce laser efficiency at higher pressures. Compared to the 4.37 μm component, the 4.30 μm

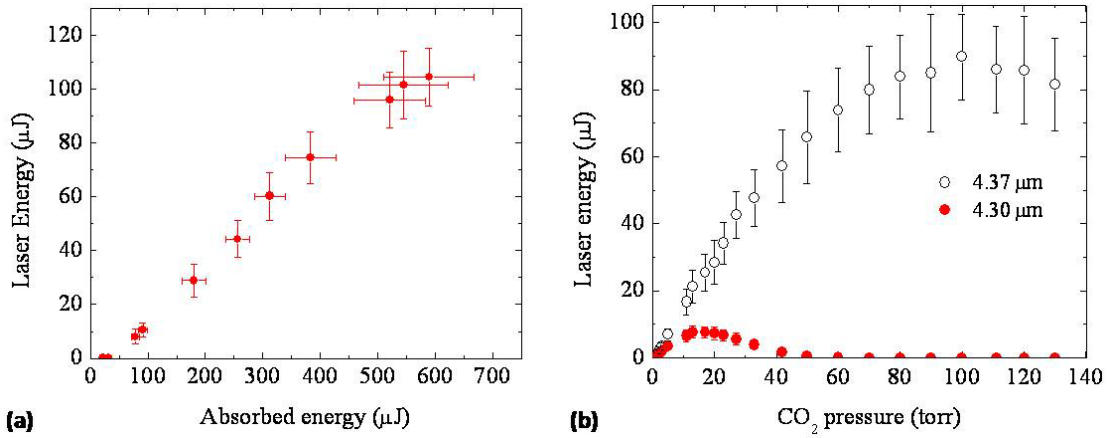

Figure 15(a). The measured CO_2-filled waveguide laser pulse energy as a function of the absorbed pump pulse energy at ~ 100 torr. (b) Energy contributions from the 4.30 μm (red-filled circles) and the 4.37 μm (unfilled circles) spectral components to the laser pulse as a function of the CO_2 gas pressure.

laser line rises slower and vanishes much more rapidly as the pressure is increased. This is because of the partial overlap of the 4.30 μm laser line with the P(30), ν_3 absorption line, resulting in re-absorption of some of the 4.30 μm light. This absorption loss is a function of the degree of overlap between the emission and re-absorption lines whose widths are pressure dependent, giving rise to a much different overall pressure dependence of the 4.30 μm laser component.

D. Conclusions

We have now demonstrated and begun to characterize mid-IR optically pumped gas lasers from both acetylene and HCN gas contained within HC-PCFs. Furthermore we have demonstrated that metal-coated capillaries provide a suitable and convenient test bed to explore gas-filled fiber lasers operating at wavelengths beyond 4 μm, where suitable HC-PCFs do not yet exist. Many interesting effects, including long (~ 30 ns) laser-to-pump pulse delays and pressure dependent spectral contributions to the mid-IR laser pulses have been observed from these gas filled fiber lasers, which require further study to more fully characterize and understand. Mid-IR laser efficiencies as high as ~ 20% have now been observed from both an acetylene-filled kagome-structured HC-PCF and a CO_2-filled silver-coated capillary. Since gas-filled HC-PCF lasers have such great potential as mid-IR sources for a multitude of applications, further experiments aimed at understanding the behavior and dependencies of these lasers is paramount to further improving laser performance.

ACKNOWLEDGEMENTS

This work was supported by the Air Force Office of Scientific Research (FA9550-08-1-0344), Army Research Office (W911NF-08-C-0106 and W911NF-08-1-0332), Joint Technology Office (W911NF-05-1-0507), Engineering and Physical Sciences Research Council, and Precision Photonics Corp. We wish to thank Kayode Oshin and Christopher Levy from the Kansas State University Chemistry Department for synthesizing the HCN.

REFERENCES

[1] Couny, F., Benabid, F., Roberts, P. J., Light, P. S., and Raymer, M. G., "Generation and photonic guidance of multi-octave optical-frequency combs," Science, 318(5853), 1118-1121 (2007).

[2] Benabid, F., Couny, F., Knight, J. C., Birks, T. A., and Russell, P. S., "Compact, stable and efficient all-fibre gas cells using hollow-core photonic crystal fibres," Nature, 434(7032), 488-491 (2005).

[3] Cregan, R. F., Mangan, B. J., Knight, J. C., Birks, T. A., Russell, P. St. J., and Allan, D. C., "Single-mode photonic band gap guidance of light in air," Science, 285(5433), 1537-1539 (1999).

[4] Light, P. S., Couny, F., Wang, Y. Y., Wheeler, N. V., Roberts, P. J., and Benabid, F., "Double photonic bandgap hollow-core photonic crystal fiber," Opt. Express, 17(18), 16238-16243 (2009).

[5] Jones, A. M., Nampoothiri, A. V. V., Ratanavis, A., Fiedler, T., Wheeler, N. V., Couny, F., Kadel, R. Benabid, F., Washburn, B. R., Corwin, K. L., and Rudolph, W., "Mid-infrared gas filled photonic crystal fiber laser based on population inversion," Optics Express, 19(3), 2309-2316 (2011).

[6] Herzberg, G. and Spinks, J. W. T., [Molecular spectra and molecular structure], Prentice-Hall, New York, (1939).

[7] Shephard, J. D., MacPherson, W. N., Maier, R. R. J., Jones, J., Hand, D., Mohebbi, M., George, A., Roberts, P., and Knight, J., "Single-mode mid-IR guidance in a hollow-core photonic crystal fiber," Opt. Express, 13(18), 7139-7144 (2005).

[8] Degnan, J. J., and Hall, D. R., "Finite aperture waveguide laser resonators," IEEE Journal of Quantum Electronics, QE 9(9), 901-910 (1973).

[9] Marcatili, E. A. J., and Schmeltzer, R. A., "Hollow metallic and dielectric waveguides for long distance optical transmission and lasers," Bell System Technical Journal, 43(4P2), 1783-1809 (1964).

Mid-infrared gas filled photonic crystal fiber laser based on population inversion

Andrew M. Jones[1], A. V. Vasudevan Nampoothiri[2], Amarin Ratanavis[2], Tobias Fiedler[2], Natalie V. Wheeler[3], François Couny[3], Rajesh Kadel[1], Fetah Benabid[3], Brian R. Washburn[1], Kristan L. Corwin[1*] and Wolfgang Rudolph[2]

[1]Department of Physics, Kansas State University, Manhattan, KS 66506, USA
[2]Department of Physics, University of New Mexico, Albuquerque, NM 87131, USA
[3]Centre for Photonics and Photonic Materials, Department of Physics, University of Bath, BA2, 7AY, UK.
[*]corwin@phys.ksu.edu

Abstract: We demonstrate for the first time an optically pumped gas laser based on population inversion using a hollow core photonic crystal fiber (HC-PCF). The HC-PCF filled with $^{12}C_2H_2$ gas is pumped with ~ 5 ns pulses at 1.52 μm and lases at 3.12 μm and 3.16 μm in the mid-infrared spectral region. The maximum measured laser pulse energy of ~ 6 nJ was obtained at a gas pressure of 7 torr with a fiber with 20 dB/m loss near the lasing wavelengths. While the measured slope efficiencies of this prototype did not exceed a few percent due mainly to linear losses of the fiber at the laser wavelengths, 25% slope efficiency and pulse energies of a few mJ are the predicted limits of this laser. Simulations of the laser's behavior agree qualitatively with experimental observations.

OCIS codes: (140.4130) Molecular gas lasers; (140.3070) Infrared and far-infrared lasers; (060.5295) Photonic crystal fibers.

References and links

1. R. Colombelli, K. Srinivasan, M. Troccoli, O. Painter, C. F. Gmachl, D. M. Tennant, A. M. Sergent, D. L. Sivco, A. Y. Cho, and F. Capasso, "Quantum cascade surface-emitting photonic crystal laser," Science **302**, 1374-1377 (2003).
2. J. Faist, F. Capasso, D. L. Sivco, C. Sirtori, A. L. Hutchinson, and A. Y. Cho, "Quantum cascade laser," Science **264**, 553-556 (1994).
3. R. F. Curl, F. Capasso, C. Gmachl, A. A. Kosterev, B. McManus, R. Lewicki, M. Pusharsky, G. Wysocki, and F. K. Tittel, "Quantum cascade lasers in chemical physics," Chem. Phys. Lett. **487**, 1-18 (2010).
4. J. E. McCord, H. C. Miller, G. Hager, A. I. Lampson, and P. G. Crowell, "Experimental investigation of an optically pumped mid-infrared carbon monoxide laser," IEEE J. Quantum Elect. **35**, 1602-1612 (1999).
5. J. E. McCord, A. A. Ionin, S. P. Phipp, P. G. Crowell, A. I. Lampson, J. K. McIver, A. J. W. Brown, and G. D. Hager, "Frequency-tunable optically pumped carbon monoxide laser," IEEE J. Quantum Elect. **36**, 1041-1052 (2000).
6. H. C. Miller, D. T. Radzykewycz, and G. Hager, "An optically pumped midinfrared HBr laser," IEEE J. of Quantum Elect. **30**, 2395-2400 (1994).
7. A. V. V. Nampoothiri, A. Ratanavis, N. Campbell, and W. Rudolph, "Molecular C_2H_2 and HCN lasers pumped by an optical parametric oscillator in the 1.5-μm band," Opt. Express **18**, 1946-1951 (2010), http://www.opticsinfobase.org/oe/abstract.cfm?URI=oe-18-3-1946.
8. T. Y. Chang and T. J. Bridges, "Laser action at 452, 496, and 541 μm in optically pumped CH_3F," Opt. Comm. **1**, 423-426 (1970).
9. T. Y. Chang and O. R. Wood, "An optically pumped CO_2 laser," IEEE J. Quantum Elect. **8**, 598 (1972).
10. H. R. Schlossberg and H. R. Fetterman, "Optically pumped vibrational transition laser in OCS," Appl. Phys. Lett. **26**, 316-318 (1975).
11. T. Ehrenreich, B. Zhdanov, T. Takekoshi, S. P. Phipps, and R. J. Knize, "Diode pumped cesium laser," Electron. Lett. **41**, 415-416 (2005).
12. C. S. Kletecka, N. Campbell, C. R. Jones, J. W. Nicholson, and W. Rudolph, "Cascade lasing of molecular HBr in the four micron region pumped by a Nd:YAG laser," IEEE J. Quantum Elect. **40**, 1471-1477 (2004).
13. F. Benabid, J. C. Knight, G. Antonopoulos, and P. S. J. Russell, "Stimulated Raman scattering in hydrogen-filled hollow-core photonic crystal fiber," Science **298**, 399-402 (2002).
14. A. R. Bhagwat and A. L. Gaeta, "Nonlinear optics in hollow-core photonic bandgap fibers," Opt. Express **16**, 5035-5047 (2008), http://www.opticsinfobase.org/oe/abstract.cfm?URI=oe-16-7-5035.
15. F. Benabid, G. Bouwmans, J. C. Knight, P. St Russell, and F. Couny, "Ultrahigh efficiency laser wavelength conversion in a gas-filled hollow core photonic crystal fiber by pure stimulated rotational Raman scattering in molecular hydrogen," Phys. Rev. Lett. **93**, 123903 (2004).
16. F. Couny, F. Benabid, P. J. Roberts, P. S. Light, and M. G. Raymer, "Generation and photonic guidance of multi-octave optical-frequency combs," Science **318**, 1118-1121 (2007).
17. R. F. Cregan, B. J. Mangan, J. C. Knight, T. A. Birks, P. S. Russell, P. J. Roberts, and D. C. Allan, "Single-mode photonic band gap guidance of light in air," Science **285**, 1537-1539 (1999).
18. J. D. Shephard, W. N. MacPherson, R. R. J. Maier, J. D. C. Jones, D. P. Hand, M. Mohebbi, A. K. George, P. J. Roberts, and J. C. Knight, "Single-mode mid-IR guidance in a hollow-core photonic crystal fiber," Opt. Express **13**, 7139-7144 (2005), http://www.opticsinfobase.org/oe/abstract.cfm?URI=oe-13-18-7139.
19. P. S. Light, F. Couny, Y. Y. Wang, N. V. Wheeler, P. J. Roberts, and F. Benabid, "Double photonic bandgap hollow-core photonic crystal fiber," Opt. Express **17**, 16238-16243 (2009), http://www.opticsinfobase.org/oe/abstract.cfm?URI=oe-17-18-16238.
20. J. v. Neumann and E. Wigner, "Über merkwürdige diskrete Eigenwerte," Phys. Z. **30**, 465 (1929).

21. F. Benabid, F. Couny, J. C. Knight, T. A. Birks, and P. S. Russell, "Compact, stable and efficient all-fibre gas cells using hollow-core photonic crystal fibres," Nature **434**, 488-491 (2005).
22. J. D. Shephard, J. D. C. Jones, D. P. Hand, G. Bouwmans, J. C. Knight, P. S. Russell, and B. J. Mangan, "High energy nanosecond laser pulses delivered single-mode through hollow-core PBG fibers," Opt. Express **12**, 717-723 (2004), http://www.opticsinfobase.org/oe/abstract.cfm?URI=oe-12-4-717.
23. M. C. Heaven, J. Han, and K. Freel, "Rotational and vibrational energy transfer from the first overtone stretch of acetylene," presented at the Sixty-fifth International Symposium on Molecular Spectroscopy, Columbus, Ohio, 21-25 June 2010.
24. HITRAN database, http://www.cfa.harvard.edu/HITRAN/.
25. W. C. Swann and S. L. Gilbert, "Pressure-induced shift and broadening of 1510-1540-nm acetylene wavelength calibration lines," J. Opt. Soc. Am. B **17**, 1263-1270 (2000).
26. J. W. Dawson, M. J. Messerly, R. J. Beach, M. Y. Shverdin, E. A. Stappaerts, A. K. Sridharan, P. H. Pax, J. E. Heebner, C. W. Siders, and C. P. J. Barty, "Analysis of the scalability of diffraction-limited fiber lasers and amplifiers to high average power," Opt. Express **16**, 13240-13266 (2008), http://www.opticsinfobase.org/oe/abstract.cfm?URI=oe-16-17-13240.
27. A. Ratanavis, N. Campbell, and W. Rudolph, "Feasibility study of optically pumped molecular lasers with small quantum defect," Opt. Comm. **283**, 1075-1080 (2010).

1. Introduction

The need for portable, tunable lasers in the mid-infrared (mid-IR) is compelling. This eye-safe spectral region offers high atmospheric transmission essential to applications such as remote sensing and space-based terrestrial imaging and communications. Quantum cascade lasers (QCLs) have emerged as promising mid-IR sources and have even been integrated with photonic crystal resonator structures [1]. However, QCLs typically operate from 4-10 μm [2], become multi-mode at high powers, and have thermal management challenges [3]. Optically pumped gas lasers, in which a narrow-band pump laser is resonant with the gas-phase medium, can be pumped in the near-infrared to produce mid-IR emissions [4-7], but remain bulky and cumbersome. In this paper we report on the demonstration of a new class of optically pumped gas laser based on population inversion. The gas is confined to a HC-PCF whose transmission spans several octaves to reach the mid-IR spectral region. The laser produces light near 3 μm when pumped at ~ 1.5 μm, offering a potentially robust, efficient, and compact means of producing step-tunable eye-safe mid-IR radiation well suited to a multitude of applications.

Compared to solid state laser media, gases have attractive properties including high damage thresholds, the possibility of heat dissipation through gas circulation, relatively large gain cross-sections, and emission frequencies from the near to far-infrared. A variety of optically pumped gas lasers have been demonstrated, from the earliest CH_3F [8], CO_2 [9], and OCS [10], to alkali vapor [11], CO [4, 5], HBr [6], C_2H_2 and HCN [7]. Some of these mid-IR lasers can be pumped via ro-vibrational overtones at wavelengths in the telecommunication bands where commercial pump sources are well established and readily available. Early work with HBr gas cells pumped at 1.3 μm has demonstrated lasing at ~ 4 μm with conversion efficiencies of ~ 25% [6]. More recently cascade lasing in HBr at wavelengths near 4 μm suggests that conversion efficiencies exceeding 50% are possible [12]. The main disadvantage that has limited widespread use of gas lasers and prevented their integration into many practical optical systems is the bulky, fragile packaging necessary to achieve long optical path lengths and extract appreciable laser output due to the dilute nature of gas media.

The problem of weak interaction between light and gas has been solved with the advent of gas-filled HC-PCF, whereby light and the gas phase are confined to areas on the order of 100 μm^2 over distances of tens of meters [13]. A variety of nonlinear optical phenomena [14] have been demonstrated using HC-PCF including the development of a gas-filled fiber Raman laser [15] and a multi-octave spanning Raman frequency comb [16]. HC-PCF [17] consists of a hollow, air-filled core surrounded by a periodic array of smaller holes. Two classes of HC-PCF have emerged. The first guides via a photonic bandgap [17] and has demonstrated narrow-band guidance near 3 μm [18], but not the octave-spanning guidance [19] required for this work. The second, represented by kagome HC-PCF [13], guides via a mechanism akin to Von Neumann and Wigner states [20] whereby core and cladding modes can coexist essentially without coupling to each other. As a result of this salient feature, kagome HC-PCF permits ultra-broad, multi-octave spanning spectral guidance [13], with reasonably low loss (< 1 dB/m) across a broad spectrum. These fibers can be spliced to solid-core fibers, creating compact, robust sealed gas cells that can readily be integrated into devices [21].

2. Experimental gas-filled fiber laser setup

2.1 Fiber specifics

The kagome fiber used here is the first to demonstrate multi-octave spanning guidance that includes the mid-IR; its cross section and guided modes are shown in Fig. 1a-c. The fiber is formed from high purity, low OH content (~ 0.1 ppm) fused silica using a stack and draw technique. Light out to ~ 3.4 μm is reasonably well guided in the fiber, even though fused silica exhibits strong absorption at wavelengths beyond ~ 3 μm, because the light that propagates

is mostly confined to the hollow central core. A 3-ring cladding surrounds a single-cell defect core ~ 45 μm in diameter, with excellent guidance at the pump wavelength of 1.52 μm and weak guidance near the laser wavelengths in the mid-IR. Figure 1d shows the measured and calculated fiber loss spectrum and the calculated group velocity. Standard cut-back measurements were performed to measure the wavelength dependent loss of the fiber. A broadband optical source and an optical spectrum analyzer were used at wavelengths below 1.75 μm. The data at 3.16 μm was taken using the output of an optical parametric oscillator (OPO) coupled through the fiber and detected by a PbSe photodetector. The measured fiber

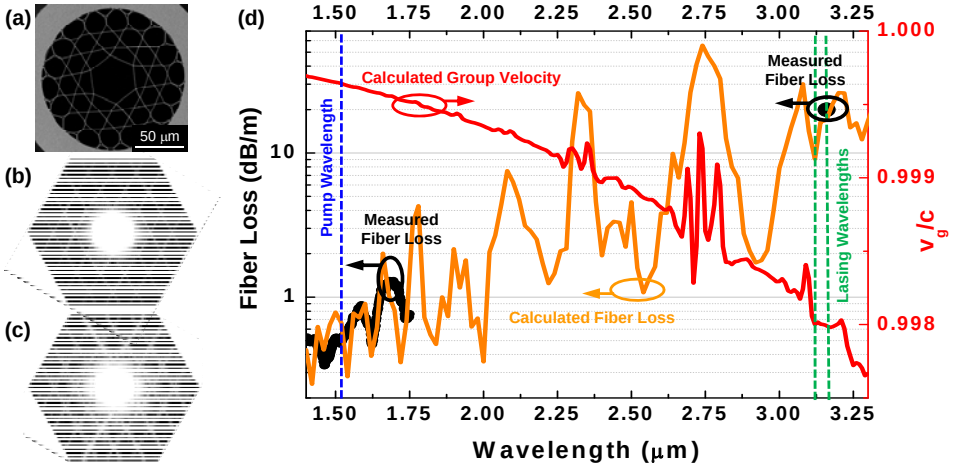

Fig. 1. Kagome HC-PCF fiber structure, guided mode profiles, and loss spectrum and group velocity. (a) Scanning electron microscope image of the cross section of the fiber used in the experiment. The diameter of the hollow core varies from 42.4 – 48.3 μm. The fiber pitch is ~ 23 μm, and the typical strut thickness is ~ 0.4 μm. Calculated core mode profiles at (b) 1.52 μm and (c) 3.12 μm. (d) Measured (black circles) and calculated (orange) fiber loss with the calculated group velocity (red).

loss is less than 0.5 dB/m near 1.5 μm and is 20 dB/m at 3.16 μm. More data points in the region beyond 1.75 μm can be taken but require a more stable OPO output mode and pulse energy while tuning the wavelength than was available. The calculated fiber loss is a result of the confinement loss of the fiber, which arises partially from the fact that the microstructured cladding region is finite in size, and partly from the intrinsic guidance mechanism of the fiber whereby there is a residual coupling between the cladding continuum modes and the guided core modes [16]. This results in a light leakage from core guided modes though the microstructured cladding into the outer bulk silica. In our work the confinement loss was calculated using finite element analysis software from JCMwave which was also used to solve the fiber modes. The measured and calculated fiber losses are in good agreement, allowing fast and accurate numerical customization and optimization of fiber loss profiles in the future.

2.2 Laser configuration

The laser setup along with a 3-μm beam profile are shown in Fig 2. The heart of the laser is the hollow PCF waveguide, which contains the gas-phase gain medium and serves as the laser cavity by guiding only emissions that fall within the guided modes of the fiber, effectively providing spectral and spatial feedback leading to coherent laser oscillation. Both ends of the kagome fiber are supported inside vacuum chambers within 1 cm of the windows, allowing light to be coupled through the evacuated fiber. Experiments were performed with 1.65-m and 0.95-m long HC-PCFs. Filling the evacuated fiber with acetylene ($^{12}C_2H_2$) gas to equilibrium pressures of up to tens of torr takes only minutes owing to the relatively large fiber core, and implies average flow rates of ~ 10^{10} molecules/s. Use of a 19-cell defect fiber with core diameters of 50-70 μm would further decrease the filling times and allow even faster flow rates. BK7 glass optics couple in pump light at ~ 1.5 μm, while CaF_2 optics couple light out. The laser is pumped with an OPO producing pulses roughly 5 ns in duration with a bandwidth of about 3.5 GHz tuned to resonance with the $\nu_1 + \nu_3$ (R7) ro-vibrational transition in $^{12}C_2H_2$, λ = 1521.06 nm. The pump pulse energy incident on the fiber is kept below 100 μJ to avoid damage [22]. Polished germanium wafers filter transmitted pump light from mid-IR laser pulses exiting the fiber. A fast InGaAs photodetector measures pump pulse energy while a fast HgCdTe photodetector observes mid-IR pulses.

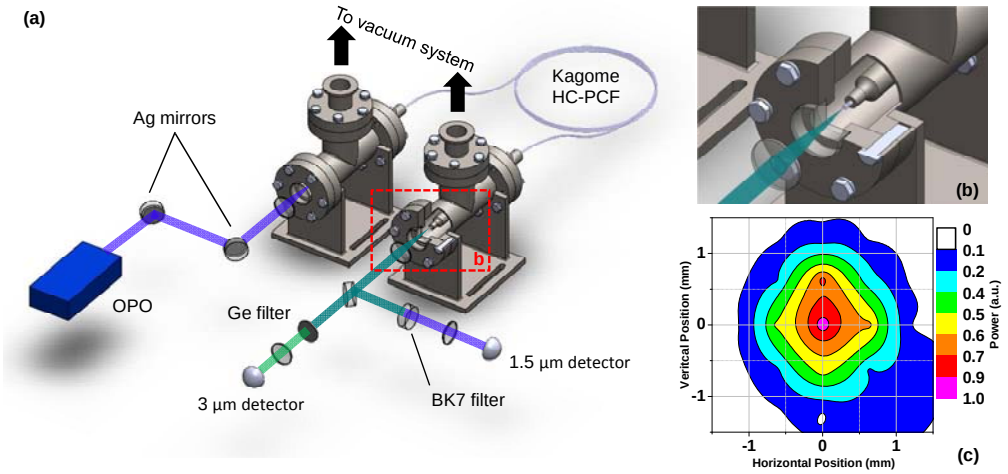

Fig. 2. Experimental setup and laser beam profile. (a) Pulses from an OPO with a center wavelength of ~ 1.5 μm and 5 ns duration (shown in blue) are coupled into a kagome structured HC-PCF containing low pressure acetylene gas. Pump radiation is absorbed by the gas and laser radiation is detected from ro-vibrational transitions at wavelengths in the mid-IR (shown in green). Laser energy is filtered from pump energy by a polished germanium wafer and detected by a fast, room-temperature HgCdTe photovoltaic detector. (b) Close-up showing a fiber end suspended in a vacuum chamber. (c) Far-field mode profile: power of the collimated 3 μm beam passing through a 750-μm diameter circular aperture as the aperture is scanned transverse to the beam.

3. Experimental results and discussion

Pump pulses excite acetylene molecules from the $J = 7$ rotational state of the vibrational ground state to the $J = 8$ rotational state of the $v_1 + v_3$ vibrational manifold (Fig. 3 inset). Acetylene molecules can then leave this excited state via radiative transitions to the v_1 vibrational state with corresponding emission wavelengths in the 3 μm region. Alternatively, molecules initially in the excited state may exchange energy nonradiatively through intermolecular collisions and collisions with the fiber wall, processes that can decrease the overall laser efficiency. The relative contribution of wall collisions is expected to be small at pressures above 2 torr, where the calculated mean free path of gas molecules is < 20 μm. Just as in the free space acetylene laser [7], two peaks in the laser spectrum are seen at 3.12 μm and 3.16 μm (Fig. 3). These peaks correspond to the dipole allowed transitions ($\Delta J = \pm 1$) from the $J = 8$, $v_1 + v_3$ excited state to the $J = 7$ and $J = 9$ rotational states of the v_1 vibrational state. The absence of any other peaks indicates insufficient time for molecules in the excited state to rotationally mix through intermolecular collisions before the onset of lasing and vibrational relaxation. Measured total removal rates from the upper pump level are ~ 10^{-9} cm^3s^{-1} [23].

Figure 4 shows laser pulse energies measured at various acetylene gas pressures for a fixed pump energy. The maximum laser pulse energy is ~ 6 nJ measured at an acetylene pressure of 7 torr. Delay between the transmitted pump and laser pulses does not exceed 5 ns. Laser pulse durations were observed to be between ~ 3 ns and 5 ns. The lasing threshold occurs at about 200 nJ of coupled pump pulse energy and varies with pressure. The slope efficiency is only ~ 1% in comparison with about 10% from the free space acetylene laser [7], but can be improved by reducing the fiber attenuation at the laser wavelength through optimization of the fiber length and pitch. Neglecting relaxation processes, the maximum possible slope efficiency for this laser is 25% and is a result of saturating both the pump and lasing transitions. In the limit of lossless fiber and 25% efficiency the ultimate achievable pulse energies to expect from these lasers should be limited by the fiber damage threshold. Damage fluences for 8-ns pulses at 1064 nm on the order of 100 J/cm^2 were observed for the cladding in HC-PCFs [20], which roughly corresponds to the critical fluence of bulk fused silica. In contrast, a 25 times higher fluence was demonstrated for the guided mode [20]. If we assume that the damage fluence scales as the square root of the pulse duration and is rather wavelength independent we obtain an estimate for the maximum pump energy that can be coupled into our fiber on the order of 10 mJ, which

would result in a maximum laser energy of a few mJ. This energy limit can be increased through the use of larger core fibers, longer pulse durations and more efficient lasing schemes.

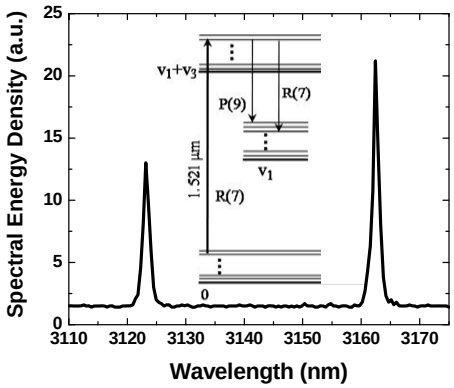

Fig. 3. Spectrum of the acetylene-filled PCF laser. The laser spectrum was taken using a grating spectrometer with ~ 1 nm resolution. The two peaks correspond to transitions from the $J = 8$, $v_1 + v_3$ pump state to the $J = 7$ and $J = 9$, v_1 state, corresponding to wavelengths of 3123.2 nm and 3162.4 nm, respectively. The inset shows pertinent transitions on an energy level diagram.

4. Modeling results

We use a simple model to qualitatively predict the trends observed in the experiment. The model system is comprised of only three states: a ground state, the pumped excited state, and a terminal excited state with no direct path for population to transfer to or from the ground state during our time scale of interest. The absorption cross-section for the pump transition is estimated as 7.7×10^{-18} cm^2 [24]. Since data for the stimulated emission cross-section for the lasing transition is not available, we assume that it is of the same order of magnitude as that for the $v_3 \rightarrow v_0$ transition, which is estimated to be ~ 2.2×10^{-16} cm^2 using the known Einstein A coefficient [24]. A Gaussian pump pulse 5 ns long and 2 GHz in bandwidth spectrally centered on resonance with the gas at 1.52 μm enters the fiber, creating a population inversion. The laser pulse develops from spontaneous emission and co-propagates with the pump; linear fiber losses are accounted for. The model predicts an optimum pressure, experimentally observed in Fig. 4, which is a function of the fiber length and pump energy. The optimum pressure essentially occurs when a given pump pulse energy just creates enough gain to balance the fiber loss at the end of the fiber. Any further increase in pressure causes additional pump absorption, resulting in more loss than gain before the fiber end. A smaller pressure dependent effect arises from the linewidth of the pump transition (~ 1 GHz at 7 torr [25]).

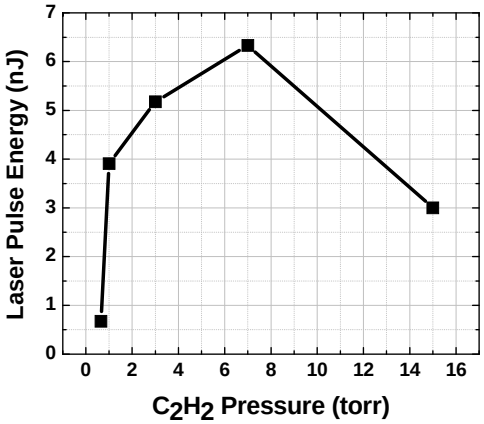

Fig. 4. Measured dependence of laser pulse energy on gas pressure. Laser pulse energy increases with $^{12}C_2H_2$ gas pressure and peaks at ~ 6 nJ at 7 torr. The pump pulse energy launched into the 1.65 m long fiber was about 1 μJ.

The measured and predicted laser pulse energies as a function of pump pulse energy are shown in Fig. 5a and Fig. 5b respectively. The experimental and calculated data are in good qualitative agreement, showing exponential-like small signal gain followed by the onset of saturation as the pump pulse begins to saturate the gas absorption at the end of the fiber. Only relative comparisons between experiment and calculation can be made because the exact fiber-to-free space coupling efficiencies are not known. Cut-back measurements to determine the actual efficiencies are complicated by time-dependent fluctuations in the spatial mode and center frequency of pump pulses from the OPO. Mid-IR laser output as a function of fiber length as predicted by the model is shown in Fig. 5c. When pumping at 6 μJ (solid curves), the first knee present in the laser energy curve occurs when the saturated gain approximately equals the linear fiber loss for the laser radiation. The plateau in the output power persists while the pump is able to maintain (saturated) gain that equals the linear fiber loss for the laser radiation, ending when the depleted pump cannot maintain sufficient population inversion. Figure 5d-f show the evolution of pump (blue) and laser (green) pulse power calculated at different positions along the length of the fiber for a launched pump (gray) pulse energy of 6 μJ. Initially the laser pulse develops at the leading edge of the undepleted pump pulse (Fig. 5d). As the leading edge of the pump is absorbed and saturates the transition, the positive net gain window shifts towards later times during the pump pulse. As a result the laser pulse broadens and its center moves backwards (Fig. 5e). At long fiber lengths the pump is almost completely absorbed and the laser pulse energy begins to decrease as the pump can no longer sustain the inversion necessary to compensate the fiber loss (Fig. 5f). Additionally, the temporal width of the laser pulse broadens as it propagates along the fiber and never exceeds the 5-ns duration of the launched pump pulse.

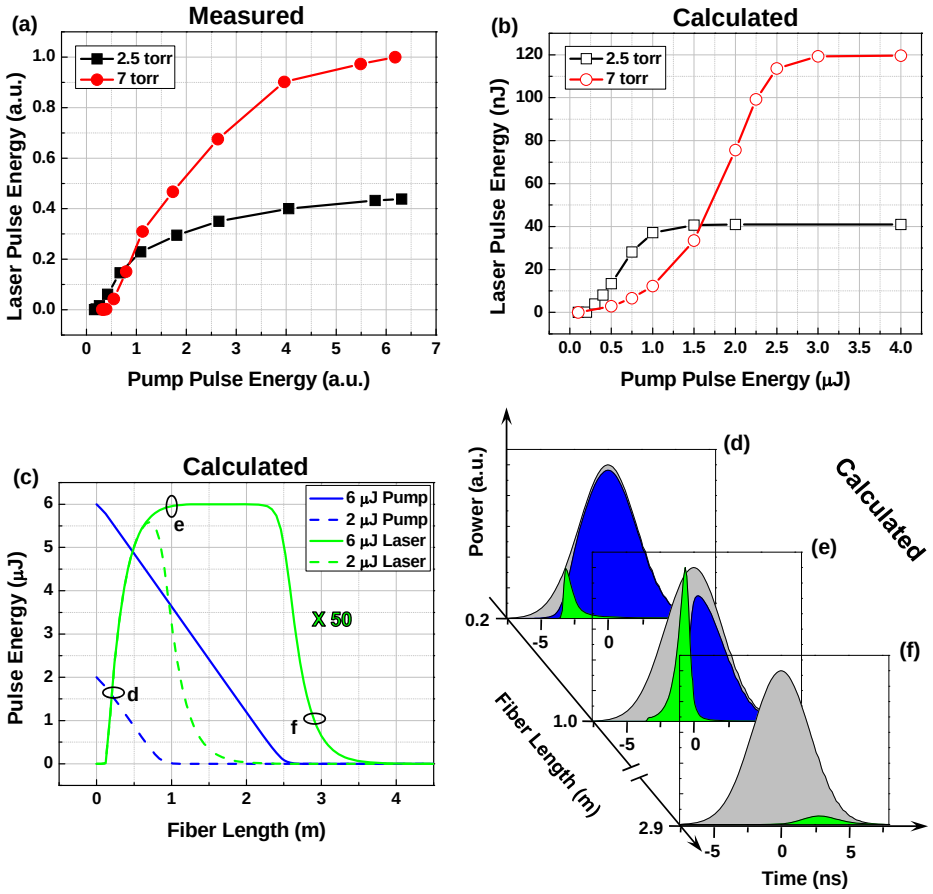

Fig. 5. Experimental and calculated laser pulse energy dependence on pump energy and fiber length. Laser pulse energy (a) measured and (b) calculated for various levels of pump pulse energy coupled into a 0.9 m long fiber containing $^{12}C_2H_2$ at pressures of 2.5 and 7 torr. (c) The calculated laser (green curves) and pump (blue curves) pulse energies at different positions along the fiber length containing 7 torr of $^{12}C_2H_2$ gas for two different launched pump pulse energies; the laser energy is multiplied by a factor of 50. (d-f) The calculated temporal profiles of the laser (green), and transmitted pump (blue) pulses along with the launched pump (gray) pulse at several positions along the fiber, where the laser power is scaled up by a factor of 5.5.

5. Conclusions

Realization of the first gas fiber laser based on population inversion holds great promise for coherence generation applications as well as for engineering high power, portable and robust, all fiber mid-IR sources in the future. One can effectively engineer gas-filled fiber laser sources at numerous wavelengths difficult to obtain with other technologies by carefully selecting the gas and designing the optical fiber. The gas must absorb at wavelengths where inexpensive, high-power pump sources exist, and lase at a wavelength of interest; the fiber should be highly transmissive at both the pump and laser frequencies while suppressing lasing on unwanted transitions. While the performance of solid core fiber lasers at high powers can be limited by the onset of nonlinear processes such as Brillouin and Raman scattering [26], gas-filled HC-PCF lasers can be expected to surpass these limits and have higher thresholds for damage, because no glass or other host material is present in the high intensity region of the propagating modes. Thus, phase-locking multiple gas-filled fiber lasers together may achieve higher ultimate powers than can be realized with solid-core systems. Sealing the fiber permits an all-fiber device, facilitating easy integration into optical systems. Continuous-wave (CW) operation of the laser is paramount for use in many potential applications. This will require fast repopulation of the

ground state, which may favor asymmetric molecules or require buffer gases for tailored energy transfer. The addition of buffer gases may speed rotational mixing of the excited state population, remove population from unwanted vibrational states, and accelerate heat dissipation. Furthermore, extremely efficient molecular CW lasers with very small quantum defects [27] similar to alkali vapor lasers seem feasible with PCFs.

6. Acknowledgements

This work was supported by the Air Force Office of Scientific Research (FA9550-08-1-0344), Army Research Office (W911NF-08-C-0106 and W911NF-08-1-0332), National Science Foundation (PHY-0722622), Joint Technology Office (W911NF-05-1-0507), Engineering and Physical Sciences Research Council (EP/E039162/1), and Precision Photonics Corp. We thank John Zavada for early discussions leading to the initial idea, P.J. Roberts for his assistance with the numerical modeling of the fiber, Neil Campbell for useful discussions, and Josh Perkins for preliminary work.

Mid-IR Fiber Lasers Based on Molecular Gas-filled Hollow-Core Photonic Crystal Fiber

Andrew M. Jones[1], A. V. Vasudevan Nampoothiri[2], Amarin Ratanavis[2], Rajesh Kadel[1], Natalie V. Wheeler[3], François Couny[3], Fetah Benabid[3], Wolfgang Rudolph[2], Kristan L. Corwin[1], and Brian R. Washburn[1]

[1]*Department of Physics, Kansas State University, Manhattan, KS 66506, USA*
[2]*Department of Physics, University of New Mexico, Albuquerque, NM 87131, USA*
[3]*Centre for Photonics and Photonics Materials, Department of Physics, University of Bath, BA2, 7AY, UK*
jonesam@phys.ksu.edu, washburn@phys.ksu.edu

Abstract: Lasing from HCN gas contained in HC-PCF is observed for the first time. Mid-IR pulses (3.15 and 3.09 μm) were generated by optically pumping at λ ~ 1.54 μm. A $^{12}C_2H_2$-filled HC-PCF molecular gas laser is also studied quantitatively.

OCIS codes: (140.4130) Molecular gas lasers; (140.3510) Lasers, fiber; (060.5295) Photonic crystal fibers

1. Introduction

Recently, we demonstrated the first time optically pumped gas laser (OPGL) based on population inversion using a hollow core photonic crystal fiber (HC-PCF) filled with $^{12}C_2H_2$ gas [1]. Here, we extend the OPGL to the first optically pumped $H^{12}C^{14}N$ gas laser in a HC-PCF. The laser produces mid-IR (3.15 and 3.09 μm) radiation by optically pumping with 1.54 μm nanosecond pulses. Furthermore, we have improved our $^{12}C_2H_2$ gas laser stability and coupling efficiency, facilitating more quantitative study and comparison with a theoretical model. We have also examined the laser polarization, the effects of buffer gas, and the effects of higher acetylene pressure on the laser performance. These studies establish the HC-PCF based laser cavity as a universal laser configuration for many optically pumped molecular gas lasers with low threshold combined with the potential for high slope efficiency and coherent beam combination among multiple fibers.

Optically pumped gas lasers in HC-PCF offer many advantages to more traditional gas laser geometries that use gas cells. Kagome structured HC-PCF can serve as a cavity that permits long interaction lengths between the pump and gas medium leading to a confinement area the order of 100 μm^2 over distances of tens of meters. Furthermore, the kagome HC-PCF permits ultra-broad, multi-octave spanning spectral guidance [2], with reasonably low loss (<0.5 dB/m across a broad spectrum, and can be spliced to solid-core fibers, creating compact, robust sealed gas cells [Fetah 2005]. Furthermore, there is a wide selection of molecular gases that can be pumped in near 1.5 μm [3] to produce mid-IR lasing.

2. Experimental Setup and Characterization of the $^{12}C_2H_2$ Laser

The experimental setup used for both molecular gas lasers is shown in Fig. 1a. An optical parametric amplifier (OPA) was used to amplify a seed laser produced from a tunable C-band continuous wave (CW) laser. Pulses 1 ns in duration from a Nd:YAG laser were mixed with the CW laser in a nonlinear crystal to produce 20 μJ pulses at ~1.5 μm. To pump the C_2H_2 laser, the OPA was tuned to 1.532 μm corresponding to pumping of the

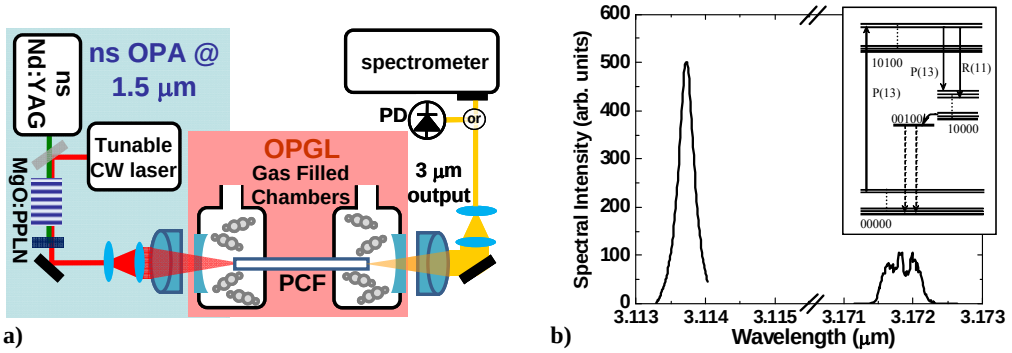

Fig. 1. a) Setup used for both the HCN and C_2H_2 gas lasers. b) The spectrum of the C_2H_2 laser pumped at 1.532 μm, where the two peaks correspond to transitions from the $J = 12$, $\nu_1 + \nu_3$ pump state to the $J = 11$ and $J = 12$, ν_1 state. Inset: C_2H_2 energy transitions.

$\nu_1+\nu_3$ (P(13)) transition in C_2H_2. The pulses were coupled (with 50% efficiency) into a vacuum chamber containing a single-cell kagome structured optical fiber of 33 cm in length [2]. This kagome fiber exhibits strong guiding in the

near-IR pump region (loss ~0.75 dB/m) and weak guiding behavior at 3 μm (loss ~20 dB/m). The spectral and temporal measurements of the mid-IR output were recorded with a spectrometer and fast photodiode respectively.

We performed a series of quantitative measurements of slope efficiency and the effect of a buffer gas on the C_2H_2 laser. Figure 2a shows the output mid-IR energy as a function of absorbed near-IR pump. Here, the optimal pressure was 31 torr. The effect of collisions with buffer gas on the C_2H_2 laser efficiency was examined using the experiment described in Ref. [1] for varying active gas/buffer gas mixtures. For these measurements, C_2H_2 pressure was kept constant at 7 torr. Helium (He) was used as the buffer gas. Figure 2b shows the measured laser output as a function of input pump energy for various He pressures. It was seen that the addition of buffer gas increases the lasing threshold and reduces the laser efficiency. The observed reduction in efficiency could be attributed to increased vibrational relaxation and reduced pump absorption due to pressure broadening.

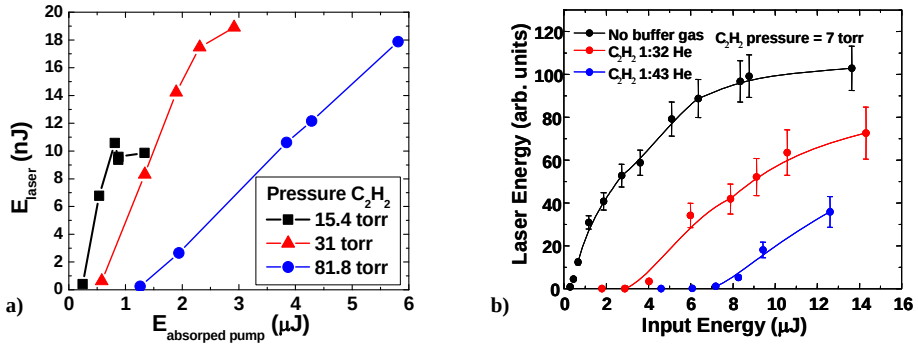

Fig. 2. a) C_2H_2 laser output energy as a function of absorbed pump energy for different gas pressures. b) Laser He buffer gas pressure dependence using the C_2H_2 filled HC-PCF laser configuration reported in Ref. [1]. Solid line is a guide to the eye.

3. Demonstration of Lasing in a $H^{12}C^{14}N$ filled HC-PCF

The above experiment was used to demonstrate lasing in a $H^{12}C^{14}N$ filled HC-PCF. The fiber in Fig. 1a was filled with HCN gas and pumped at 1.541 μm, exciting the P(10) state in the $2\nu_1$ band (overtone of the C-H stretch). Lasing at 3.147 and 3.091 μm was measured corresponding to the R(8) and P(10) states in the ν_1 band. We are currently investigating the dependence of output power and slope efficiency as a function of HCN gas pressure. This work shows that the HC-PCF laser format can be use for multiple molecular gases to generate mid-IR radiation.

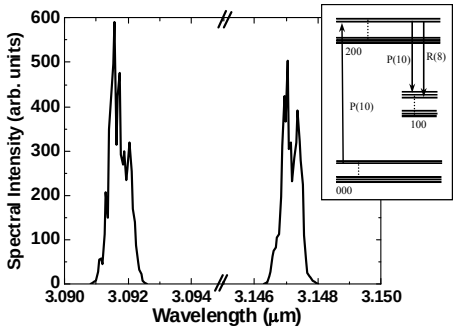

Fig. 3. The spectrum of the HCN laser pumped at 1.541 μm; the two peaks correspond to transitions from the $J = 9$, $2v_1$ pump state to the $J = 8$ and $J = 10$, v_1 state. The gas pressure was 12.8 and 18.8 torr. Inset: HCN energy transitions.

4. Acknowledgements

This work was supported by the Air Force Office of Scientific Research (FA9550-08-1-0344), Army Research Office (W911NF-08-C-0106 and W911NF-08-1-0332), Joint Technology Office (W911NF-05-1-0507), Engineering and Physical Sciences Research Council, and Precision Photonics Corp. We wish to thank Kayode Oshin and Christopher Levy from the Kansas State University Chemistry Department for synthesizing the HCN.

5. References

[1] A. M. Jones, V. V. Nampoothiri, A. Ratanavis, R. Kadel, N. Wheeler, F. Couny, F. Benabid, W. Rudolph, B. R. Washburn, and K. L. Corwin, "C_2H_2 Gas Laser Inside Hollow-Core Photonic Crystal Fiber Based on Population Inversion," in *Proceedings of Conference of Lasers and Electro-optics*, 2010)

[2] F. Benabid, J. C. Knight, G. Antonopoulos, and P. S. J. Russell, "Stimulated Raman Scattering in Hydrogen-Filled Hollow-Core Photonic Crystal Fiber," Science 298, 399 (2002).

[3] A. V. V. Nampoothiri, A. Ratanavis, N. Campbell, and W. Rudolph, "Molecular C_2H_2 and HCN lasers pumped by an optical parametric oscillator in the 1.5-μm band," Opt. Express 18, 1946-1951 (2010).

C_2H_2 Gas Laser Inside Hollow-Core Photonic Crystal Fiber Based on Population Inversion

Andrew M. Jones[1], A. V. Vasudevan Nampoothiri[2], Amarin Ratanavis[2], Rajesh Kadel[1], Natalie V. Wheeler[3], François Couny[3], Fetah Benabid[3], Wolfgang Rudolph[2], Brian R. Washburn[1], and Kristan L. Corwin[1]

[1]*Department of Physics, Kansas State University, Manhattan, KS 66506, USA*
[2]*Department of Physics, University of New Mexico, Albuquerque, NM 87131, USA*
[3]*Centre for Photonics and Photonics Materials, Department of Physics, University of Bath, BA2, 7AY, UK*
jonesam@phys.ksu.edu, corwin@phys.ksu.edu

Abstract: Lasing from population inversion is demonstrated from gas contained in a hollow-core kagome structured photonic crystal fiber. Laser pulses in the mid-IR (3.1-3.2 μm) were generated by optically pumping at λ ~ 1.5 μm.

OCIS codes: (140.4130) Molecular gas lasers; (140.3510) Lasers, fiber; (060.5295) Photonic crystal fibers

1. Introduction

We demonstrate what we believe is the first optically pumped gas laser (OPGL) based on population inversion in a hollow core photonic crystal fiber (HC-PCF). The laser produces mid-IR (3.1-3.2 μm) lasing by optically pumping with 1.5 μm, nanosecond pulses. The laser has many of the advantages of optically pumped gas lasers (OPGLs), including high damage thresholds and the potential for coherent emission from mutually incoherent pump sources. Furthermore, OPGLs with molecular gases offer a variety of mid-IR wavelengths [1-2] specifically in the eye-safe wavelengths within the atmospheric transmission window. Creating an OPGL inside hollow fiber has the added advantage of confining the pump and laser light over long interaction lengths in a compact configuration. The feasibility of implementing molecular OPGLs inside a waveguide has been previously examined [3]. Many nonlinear optical phenomena have been studied in gas-filled hollow optical fibers, including the demonstration of a Raman laser [4]. Indeed, the kagome structured fiber employed there offers very broad guiding bandwidths, well suited for the present laser in which the pump and lasing wavelengths differ by nearly a factor of two.

2. Setup for the OPGL Inside HC-PCF

In this initial demonstration of a fiber OPGL, nanosecond pulses excite acetylene gas inside HC-PCF. This approach is motivated by an OPGL based on acetylene vapor inside a glass cell that demonstrated large optical gain near 3 μm [3]. The experiment is shown schematically in Fig. 1a.

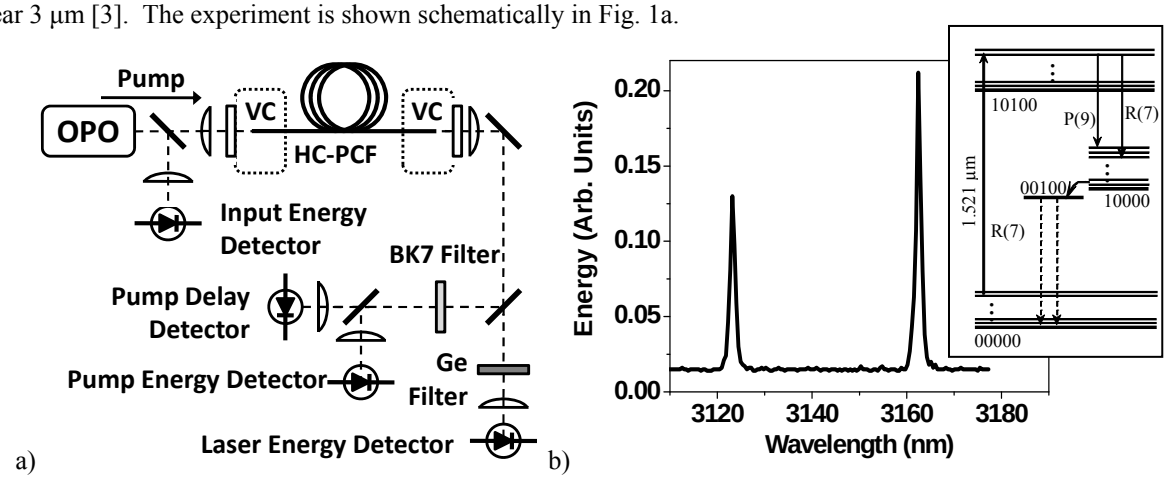

Fig. 1: a) Fiber OPGL setup. The acetylene filled HC-PCF is pumped using a nanosecond OPO. Incident pump energy, pump energy through the fiber, mid-IR laser pulse energy, and pump-to-laser pulse delay are monitored simultaneously. A germanium wafer transmits mid-IR laser pulses while attenuating pump pulses to below the noise level of the HgCdTe laser energy detector. A BK7 window is used to absorb mid-IR laser energy before the pump energy and timing detectors. b) Spectrum of laser output when C_2H_2 pressure was ~ 7 torr. Inset: Simplified energy level diagram of C_2H_2 showing the pump and two laser transitions.

An optical parametric oscillator (OPO) is used as the pulsed pump source, and its output pulses were typically 5 – 6 ns in duration with average pulse energies of ~ 5 mJ. The OPO was tuned to resonance with the $\nu_1 + \nu_3$ (R7) transition in $^{12}C_2H_2$, λ = 1521.06 nm. These pulses were directed into a vacuum chamber containing a single-cell kagome structured optical fiber of 1.65 m length, similar to that employed in Ref. [4]. This kagome fiber exhibits

strong guiding in the near IR pump region (loss ~ 0.75 dB/m) and weak guiding behavior near 3 μm (~ 20 dB/m), as calculations suggest. The gain of the laser is sufficient that no cavity was required, in spite of the large loss in the lasing band.

3. Characterization of the Laser Output

Spectral output from the OPGL, shown in Fig. 1b for ~ 7 torr acetylene gas pressure, contains two peaks located near 3.12 μm and 3.16 μm respectively, corresponding to (R7) and (P9) rotational transitions between the $\nu_1 + \nu_3$ and ν_1 vibrational levels. The OPO pump, tuned to the (R7) rotational transition, moves population from the J = 7 rotational state of the ground state vibrational manifold to the J = 8 rotational state of the $\nu_1 + \nu_3$ vibrational manifold. This creates an immediate population inversion between the J = 8, $\nu_1 + \nu_3$ state and the essentially empty ν_1 vibrational state ($N_e/N_0 \sim \exp[-h\nu_1/kT] = 9 \times 10^{-8}$) resulting in the possibility of population transfer via the allowed (R7) and (P9) dipole transitions to the J = 7 and J = 9 rotational states. Pulsed laser output was observed for gas pressures between 0.5 torr and 20 torr.

Figure 2a shows the laser pulse energy output versus pump pulse energy for an acetylene pressure of 7 torr. This curve indicates the onset of saturation as the increasing pump pulse energy starts to saturate the absorption transition. At lower pressures, saturation is more pronounced. In Fig. 2b, the lasing output is plotted as a function of acetylene pressure for pump energies of 600 nJ coupled into the fiber (30 μJ incident on the fiber). The coupling efficiency was only ~ 2%, but values exceeding 50% into kagome fiber have been demonstrated. The temporal delay between the pump and laser pulses was also measured, and varied from less than 1 ns to greater than 10 ns. Shorter delays are observed when the pump power is further above threshold, when population inversion builds up more quickly. The lasing threshold, defined as the minimum pump pulse energy coupled into the fiber necessary to observe mid-IR laser output, is about 200 nJ, and varies with pressure. The slope efficiency of the laser, defined as the change in output energy divided by the change in pump energy coupled into the fiber, is a few percent.

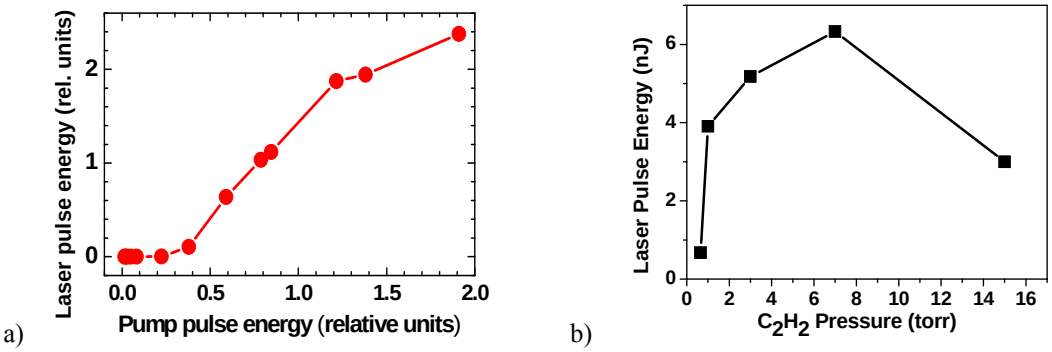

Fig. 2: a) Laser pulse output energy vs. pump pulse energy in relative units for 7 torr pressure acetylene gas. b) Mid-IR laser pulse energy vs. acetylene pressure when pumped at 30 μJ incident input pulse energy for several acetylene pressures inside the HC-PCF.

Reduction of the kagome fiber loses at the laser wavelength should substantially increase the slope efficiency and decrease the threshold. Furthermore, the addition of an optical cavity or increased kagome fiber length may also improve laser performance. Modeling efforts are ongoing. While this first demonstration uses a pulsed pump, the gas-filled fiber laser is particularly attractive for pumping with continuous wave laser sources.

4. Acknowledgements

This work was supported by the Air Force Office of Scientific Research (FA9550-08-1-0344), Army Research Office (W911NF-08-C-0106 and W911NF-08-1-0332), National Science Foundation (PHY-0722622), Joint Technology Office (W911NF-05-1-0507), Engineering and Physical Sciences Research Council, and Precision Photonics Corp.

5. References

[1] J. E. McCord, H. C. Miller, G. Hager, A. I. Lampson, and P. G. Crowell, "Experimental investigation of an optically pumped mid-infrared carbon monoxide laser," *IEEE J of Quantum Electronics,* vol. 35, pp. 1602-1612, 1999.

[2] A. Ratanavis, N. Campbell, A. V. V. Nampoothiri, and W. Rudolph, "Performance and Spectral Tuning of Optically Overtone Pumped Molecular Lasers", *IEEE J of Quantum Electronics,* vol. 45, pp. 488 2009.

[3] A.V.V. Nampoothiri, A Ratanavis, N. Campbell, and W. Rudolph, "Molecular C_2H_2 and HCN lasers pumped by an optical parametric oscillator in the 1.5-μm band", submitted to Optics Express, 2009.

[4] F. Couny, F. Benabid, P. J. Roberts, P. S. Light, and M. G. Raymer "Generation and Photonic Guidance of Multi-Octave Optical-Frequency Combs"*Science* vol. 318, pp. 1118, 2007.

Mid-IR Laser Emission from a C_2H_2 Gas Filled Hollow Core Fiber

W. Rudolph, A. V.V. Nampoothiri, A. Ratanavis, A. Jones*, R. Kadel*, B.R. Washburn*, K. L. Corwin*, N. Wheeler, F. Couny**, F. Benabid****

Department of Physics, University of New Mexico, Albuquerque, NM 87131, USA

** Department of Physics, Kansas State University, Manhattan, KS 66506, USA*

***Centre for Photonics and Photonics Materials, Department of Physics, University of Bath, BA2, 7AY, UK*

Tel: (505) 277 2081, Fax: (505) 277 1520, e-mail: wrudolph@unm.edu

ABSTRACT

We demonstrate what we believe is the first hollow fiber gas laser based on population inversion. A single-cell-defect Kagome fiber with a core diameter of about 40 microns was filled with a few torr of acetylene ($^{12}C_2H_2$). Acetylene has absorption transitions in the attractive telecommunication C band region and recently lasing was observed at about 3 microns from a gas cell when optically pumped. Pumping the gas filled fiber (1.65 m) with micro Joule pulses from a 5-ns OPO resulted in the emission of two laser lines at 3123.2 nm and 3162.4 nm. The pump (~1521 nm) was in the guiding regions of the fiber (loss ~ 0.75 dB/m) while the laser output occurred in weakly guided modes (~ 20 dB/m). This laser combines attractive features of both fiber and gas lasers, such as the confinement of the pump and laser over long interaction lengths in a compact configuration, the many possible emission wavelengths of various gases, high damage threshold, and the potential for coherent beam combining of mutually incoherent pump sources. While this first laser demonstration used a pulsed pump, the gas filled fiber laser is particularly attractive for pumping with CW laser sources.

Keywords: hollow core fiber, gas laser.

1. INTRODUCTION

Optically pumped molecular lasers (OPML) have shown to be effective wavelength converters for generating coherent radiation in the mid-infrared (mid-IR), a spectral region of great interest in applications such as remote sensing and imaging through the atmosphere. These lasers can also be potentially useful as a means to combine output of several incoherent laser sources into one coherent output beam. In order to efficiently deposit energy into the active gas whose line widths are typically smaller than a few GHz, narrow band pump sources are necessary. The recent advancements in spectral narrowing of high-power diode lasers [1,2] and fibers lasers [3] make these lasers systems well suited for the optical pumping of gases [4]. For example, diode laser pumped atomic vapor lasers have been demonstrated [5] and reached output powers exceeding 40 W [6] in the near infrared spectral region.

For beam combining it is most desirable to consider molecules whose absorption spectra match widely available narrow band fiber and/or diode lasers. In this context, we have identified molecular C_2H_2 and HCN as promising OPML candidates [7] due to their strong absorption bands in the low-loss C-band fiber telecommunications window (~ 1.5 μm) where diode and fiber optics technology is well advanced.

Conventional beam combining and power scaling in the 1.5 μm region [8] are performed using solid core fiber systems. However, power scaling in solid core fibers is often limited due to parasitic nonlinear effects e.g., stimulated Brillouin scattering [9]. One way to avoid these issues while still capitalizing on the advantages of fiber systems, such as compactness, long interaction length of pump and laser as well as confinement of modes to small volumes, is to use gas filled hollow core fibers. This concept combines advantages of fiber lasers with those of gas lasers. Gases have high damage thresholds and offer many possible (eye-safe) emission wavelengths in the atmospheric transmission window. Several nonlinear optical phenomena have been observed [10, 11] in gas filled hollow core fibers culminating in the demonstration of a Raman laser [12]. Hollow core photonic crystal fibers (HC-PCF) have shown to have transmission losses as low as 1.2 dB/km at 1.5 μm [13]. Kagome lattice based HC-PCF [11] have larger bandwidth compared to photonic band gap based hollow core fibers and exhibit multiple transmission regions with relatively low loss [14]. This makes Kagome HC-PCFs promising candidates for optically pumped gas lasers.

Recently we demonstrated lasing in the mid-IR region in $^{12}C_2H_2$ and $H^{13}CN$ when optically pumped at ~ 1.5 μm [7]. For this, we used a laser scheme based on a conventional gas cell/cavity. In this contribution we describe lasing in a C_2H_2 gas filled Kagome HC-PCF when pumped in the 1.5 μm region. For both the demonstrations, in order to attain the gain required for the lasing, a nanosecond parametric oscillator (OPO) was used as the pump source. An assessment of the cw lasing potentials of these molecules can be found in Ref. [15].

2. EXPERIMENT

The vibrational normal modes of C_2H_2 molecules and a simplified energy level diagram relevant to the optical pumping considered in this work is shown in Fig. 1.

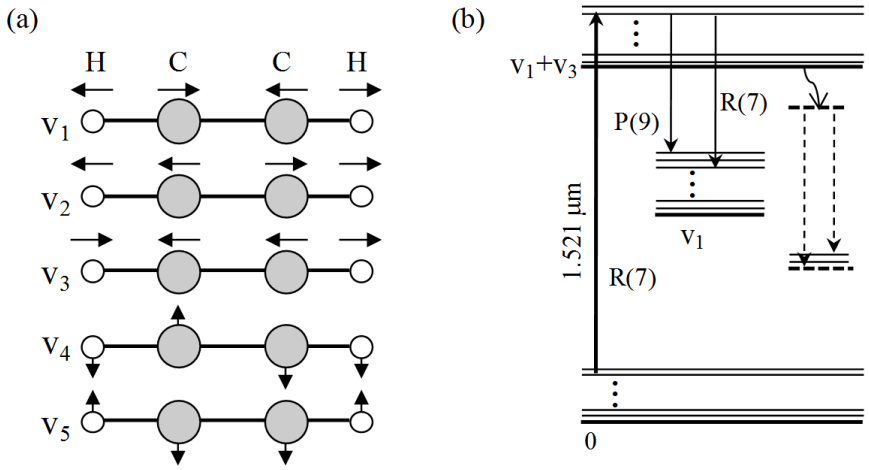

Figure 1. (a) Normal vibrational modes of C_2H_2, (b) simplified energy level diagram showing the pump and laser transitions. An R branch pump transition from $j = 7$ to $j = 8$ and observed laser transitions at about 3120 nm and 3160 nm are shown. The curly and dashed arrows represent possible vibrational relaxation from the pumped state to a lower vibrational state and subsequent laser transitions respectively (see text).

The associated vibrational energies are identified as $v_{1...5}$ for C_2H_2, and $v_{1...3}$ for HCN. For each vibrational level, there is a rotational ladder, the spacing of which to first order is given by $2B(j + 1)$, where B is the rotational constant of the particular vibrational state and j is the rotational quantum number. For example, the rotational constant for C_2H_2 for the $v_1 + v_3$ state is ~ 35.0 GHz [16]. At room temperature, according to the Boltzmann distribution, maximum population occurs in the rotational state with $j = 9$ for C_2H_2.

The experimental layout for the optically pumped gas filled hollow core fiber laser is shown in Fig. 2. A fast HgCdTe detector was employed to record the temporal profile of the laser pulses. Spectra were recorded using a near infrared (NIR) scanning spectrometer.

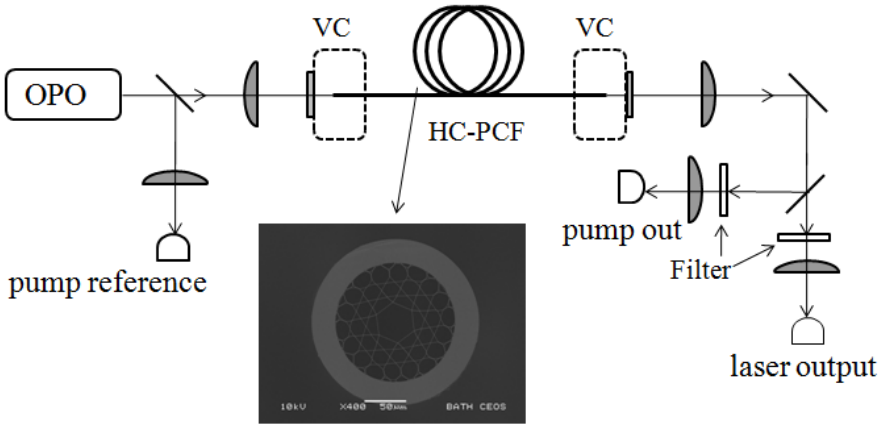

Figure 2. Schematic of optically pumped C_2H_2 filled hollow core fiber laser. HC-PCF: Kagome structured hollow core photonic crystal fiber, VC- vacuum chamber filled with C_2H_2. The bottom picture shows cross-section of the fiber.

Both ends of a 1.65-m Kagome structured hollow core fiber with a core diameter of ~ 40 µm were terminated in vacuum chambers, which were filled with a few torr of C_2H_2. The cross-section of the fiber is also shown in Fig. 2. The measured transmission loss for the fiber was ~ 0.75 dB/m at the pump wavelength and ~20 dB/m at the lasing wavelengths. The OPO was tuned to resonance with the $v_1 + v_3$ (R7) transition of C_2H_2 at ~ 1.521 µm and was coupled to the fiber using appropriate optics. Suitable filters were used to separate the laser emission from the pump radiation at the output.

3. RESULTS, INTERPRETATION AND DISCUSSION

Figure 3 shows the spectral profile of the acetylene filled HC-PCF laser for a pressure of 7 Torr. The lasing threshold, defined as the minimum pump pulse energy coupled into the fiber necessary to observe mid-IR laser

output, is about 200 nJ and varies with pressure. The laser emission shows two peaks separated by ~ 40 nm centered about 3140 nm. According to the observed laser wavelengths the two spectral components could arise from the R(7) and P(9) transitions from the terminal ($v_1 + v_3$) state to the v_1 state as indicated in Fig. 1(a).

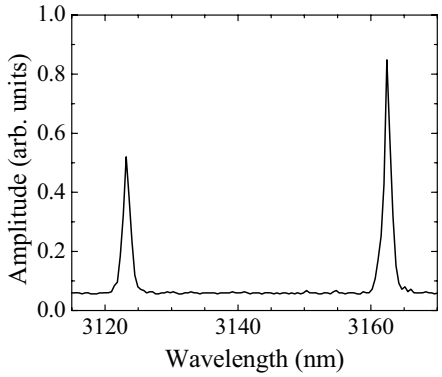

Figure 3. Spectrum of the C_2H_2 filled HC-PCF laser. The C_2H_2 pressure was 7 Torr.

The two peaks do not represent different vibration-rotation transitions from the neighboring rotational states of the terminating pump level to the same lower vibrational level; their separation would only be ~ 9 nm, estimated using the known value [16] of the rotational constant for the v_1+v_3 state. There is also the possibility that the transitions could arise from a vibrational state about 80 cm^{-1} below the upper pump level because of fast vibrational relaxation [18]. It is instructive to note the absence of any emission signature from the lower laser state v_1 to the vibrational ground state, which would be at about 3 μm. This transition is dipole forbidden [19].

Figure 4(a) shows the HC-PCF laser output as a function of pump pulse energy for two pressures, 2 and 7 Torr of acetylene. This curve indicates the onset of saturation as the increasing pump pulse energy starts to saturate the absorption transition. At lower pressures, saturation is more pronounced.

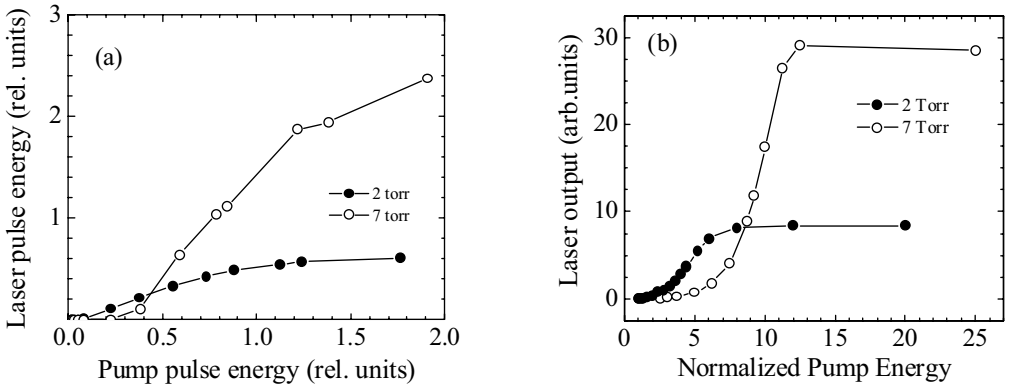

Figure 4: (a) Experimentally observed laser pulse energy as a function of pump energy, and (b) simulated laser output using a saturable absorber/amplifier model.

We have we used a simple model to qualitatively predict the trends observed in the experiment. A Gaussian pump pulse in resonance with the gas was sent through the fiber, which creates a population inversion. The laser pulse develops from spontaneous emission. In this model, both pump and probe (laser) saturate the respective transitions. The linear fiber losses were taken into account. Figure 4(b) shows the laser output as a function of input energy as predicted by the model. The results are in qualitative agreement with the experiment. The model also can be used to predict the optimum fiber length for maximum laser output.

Figure 5 shows as an example the calculated laser energy as a function of fiber length for two input energies, 500 nJ and 5 μJ, for an acetylene pressure of 7 Torr. As is evident, there is an optimum fiber length for a given input energy and pressure. This optimum arises from the interplay of pump depletion along the fiber and the relatively large linear losses at the laser wavelength in the current system.

The slope efficiency of the laser, defined as the change in output energy divided by the change in pump energy coupled into the fiber, is a few percent. In this initial demonstration, no attempt was made to optimize the laser output by finding the optimal pressure, fiber length and other parameters. Optimization of these parameters would result in higher slope efficiency. A different Kagome design with lower losses at the laser wavelength would also increase the efficiency.

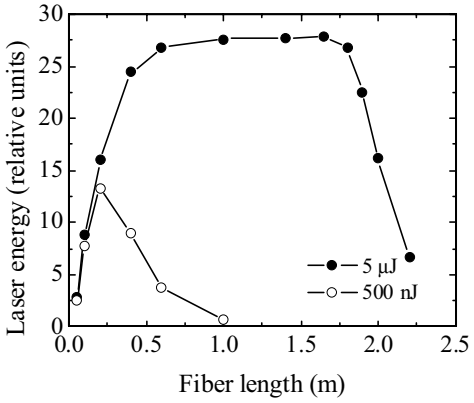

Figure 5. Calculated laser energy as a function of fiber length. The C_2H_2 pressure was 7 Torr.

In summary, we have demonstrated for the first time, mid-IR (~ 3 μm) lasing from a C_2H_2 filled HC-PCF based on population inversion when pumped at 1.5 μm. With suitable fiber bandwidths, the gas filled HC-PCF is likely to give similar results with many other molecular gases, including HCN.

ACKNOWLEDGEMENTS

The authors acknowledge support from Air Force Office of Scientific Research (FA9550-08-1-0344), Army Research Office (W911NF-08-C-0106 and W911NF-08-1-0332), National Science Foundation (PHY-0722622), Joint Technology Office (W911NF-05-1-0507), Engineering and Physical Sciences Research Council, and Precision Photonics Corp. We are grateful to Michael Heaven (Emory University) for sharing preliminary C_2H_2 spectroscopic data with us.

REFERENCES

[1] Gourevitch, G. Venus, V. Smirnov, D.A. Hostutler, and L. Glebov, *Opt. Lett.* **33**, 702-704 (2008).
[2] J.F. Sell, W. Miller, D. Wright, B.V. Zhdanov, and R.J. Knize, *Appl. Phys. Lett.* **94**, 051115-1 – 051115-3 (2009).
[3] N. Jovanovic, M. Aslund, A. Fuerbach, S. D. Jackson, G. D. Marshall, and M. J. Withford, *Opt. Lett.* **32**, 2804-2806 (2007).
[4] L. S. Meng, B. Nizamov, P. Madasamy, J. K. Brasseur, T. Henshaw, and D. K. Neumann, *Opt. Express* **14**, 10469-10474 (2006).
[5] T. Ehrenreich, B. Zhdanov, T. Takekoshi, S.P. Phipps, and R.J. Knize, *Electron. Lett.* **41**, 415-416 (2005).
[6] B.V. Zhdanov, M.K. Shaffer, and R.J. Knize, *Opt. Express* **17**, 14767-14770 (2009).
[7] A.V.V. Nampoothiri, A. Ratanavis, N. Cambell, and W. Rudolph, *Opt. Express* **18**, 1946-1951 (2010).
[8] Y. Jeong, S. Yoo, C. A. Codemard, J. Nilsson, J. K. Sahu, David N. Payne, R. Horley, P. W. Turner, Louise Hickey, A. Harker, M. Lovelady, and A. Piper, *IEEE Journal of Sel. Topics In Quantum Electron*. **13**, 573-579 (2007).
[9] J. Limpert, F. Roser, S. Klingebiel, T. Schreiber, C. Wirth, T. Peschel, R. Eberhardt, and A. Tunnermann, *IEEE Journal of Sel. Topics In Quantum Electron*. **13**, 537-545 (2007).
[10] R. Thapa, K. Knabe, M. Faheem, A. Naweed, O.L. Weaver, and K.L. Corwin, *Opt. Lett.* **31**,2489-2491 (2006).
[11] F. Benabid, J. C. Knight, G. Antonopoulos, and P. St. J. Russell, *Science* **298**, 399-402 (2002).
[12] F. Couny, F. Benabid, and P. S. Light, *Phys. Rev. Lett.* **99**, 143903-1 – 143903-4 (2007).
[13] P. J. Roberts, F. Couny, H. Sabert, B. J. Mangan, D. P. Williams, L. Farr, M. W. Mason, A. Tomlinson, T. A. Birks, J. C. Knight, and P. St.J. Russell, *Opt. Express* **13**, 236-244 (2005).
[14] F. Couny, F. Benabid, and P. S. Light, *Optics Letters* **31**, 3574-3576 (2006).
[15] A. Ratanavis, N. Campbell, and W. Rudolph, *Opt. Commun.* **283** 1075-1080 (2009).
[16] M. Herman, A. Campargue, M. I. El Idrissi, and J. Vander Auwera, *J. Phys. Chem. Ref. Data* **32**, 921-1361 (2003).
[17] W. C. Swann and S.L. Gilbert, *J. Opt. Soc. Am. B* **22**, 1749 – 1756 (2005).
[18] M.C. Heaven (private communication).
[19] G. Herzberg, *Infrared and Raman Spectra,* D. Van Nostrand Company: New York, 1945.

Optically Pumped C_2H_2 and HCN Lasers with Conventional Cavities and Based on Hollow Core Photonic Crystal Fibers

Vasudevan Nampoothiri[a], Andrew M. Jones[b], Amarin Ratanavis[a], Neil Campbell[a], Rajesh Kadel[b], Natalie Wheeler[c], François Couny[c], Fetah Benabid[c], Brian R. Washburn[b], Kristan L. Corwin[b], and Wolfgang Rudolph[a]

[a]*Department of Physics and Astronomy, University of New Mexico, Albuquerque, NM-87131*
[b]*Department of Physics, Kansas State University, Manhattan, KS 66506, USA*
[c]*Centre for Photonics and Photonics Materials, Department of Physics, University of Bath, BA2, 7AY, UK*

Abstract. Lasing in C_2H_2 and HCN are demonstrated in conventional gas cell/cavity geometries and with hollow core photonic crystal fibers when optically pumped in the 1.5 μm region by a ns optical parametric oscillator. Two lasing transitions in the mid-IR region (3 μm) are observed.

Keywords: Molecular gas lasers, Fiber lasers, Photonic crystal fibers
PACS: 42.55.Lt, 42.55.Wd

INTRODUCTION

Optically pumped molecular lasers (OPML) have shown to be effective wavelength converters for generating coherent radiation in the mid-infrared (mid-IR), a spectral region of great interest in applications such as remote sensing and imaging through the atmosphere. These lasers can also be potentially useful as a means to combine output of several incoherent laser sources into one coherent output beam. In order to efficiently deposit energy to the active gas whose line widths are typically smaller than a few GHz, narrow band pump sources are necessary. The recent advancements in spectral narrowing of high-power diode lasers [1,2] and fibers lasers [3] make these lasers systems well suited for the optical pumping of gases [4]. For example, diode laser pumped atomic vapor lasers have been demonstrated [5] and reached output powers exceeding 40 W [6] in the near infrared spectral region.

For beam combining it is most desirable to consider molecules whose absorption spectra match widely available narrow band fiber and/or diode lasers. In this context, we have identified molecular C_2H_2 and HCN as promising OPML candidates [7] due to their strong absorption bands in the low-loss C-band fiber telecommunications window (~ 1.5 μm) where diode and fiber optics technology is well advanced.

Conventional beam combining and power scaling in the 1.5 μm region [8] is performed using solid core fiber systems. However, power scaling in solid core fibers is often limited due to parasitic nonlinear effects e.g., stimulated Brillouin scattering [9]. One way to avoid these issues while still capitalizing on the advantages of fiber sys-

tems, such as compactness, long interaction length of pump and laser as well as confinement of modes to small volumes, is to use gas filled hollow core fibers. This concept combines advantages of fiber lasers with those of gas lasers. Gases have high damage thresholds and offer many possible (eye-safe) emission wavelengths in the atmospheric transmission window. Several nonlinear optical phenomena have been observed [10, 11] in gas filled hollow core fibers culminating in the demonstration of a Raman laser [12]. Hollow core photonic crystal fibers (HC-PCF) have shown to have transmission losses as low as 1.2 dB/km at 1.5 μm [13]. Kagome lattice based HC-PCF [11] have larger bandwidth compared to photonic band gap based hollow core fibers and exhibit multiple transmission regions with relatively low loss [14]. This makes HC-PCFs promising candidates for optically pumped gas lasers.

In this paper we demonstrate lasing in the mid-IR region in $^{12}C_2H_2$ and $H^{13}CN$ when optically pumped at ~ 1.5 μm. For this, we used a laser scheme based on a conventional gas cell/cavity. We also describe lasing in a C_2H_2 gas filled Kagome HC-PCF when pumped in the 1.5 μm region. For both the demonstrations, in order to attain the gain required for the lasing, a nanosecond parametric oscillator (OPO) was used as the pump source. An assessment of the cw lasing potentials of these molecules can be found in reference [15].

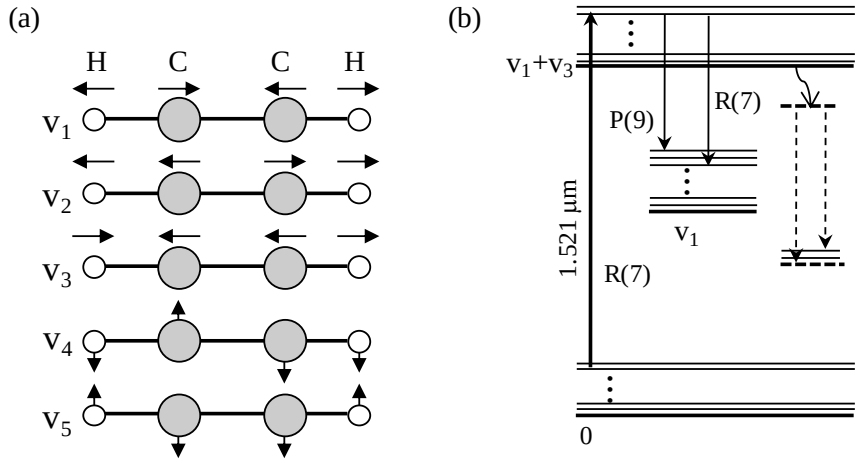

FIGURE 1. (a) Normal vibrational modes of C_2H_2, (b) simplified energy level diagram showing the pump and laser transitions. An R branch pump transition from j = 7 to j = 8 and observed laser transitions at about 3120 nm and 3160 nm are shown. The curly and dashed arrows represent possible vibrational relaxation from the pumped state to a lower vibrational state and subsequent laser transitions respectively (see text).

The vibrational normal modes of C_2H_2 and HCN molecules along with their simplified energy levels relevant to the optical pumping considered in this work is shown in Figs. 1 and 2. The associated vibrational energies are identified as $v_{1\ldots5}$ for C_2H_2, and $v_{1\ldots3}$ for HCN. For each vibrational level, there is a rotational ladder, the spacing of which to first order is given by $2B(j+1)$, where B is the rotational constant of the particular vibrational state and j is the rotational quantum number. For example, the rotational constant for C_2H_2 for the v_1+v_3 state is ~ 35.0 GHz [16], and B ~ 42.6 GHz for the $2v_3$ state of HCN [15]. At room temperature, according to the Boltzmann distribu-

tion, maximum population occurs in the rotational state with j = 9 for C_2H_2 and j = 8 for HCN.

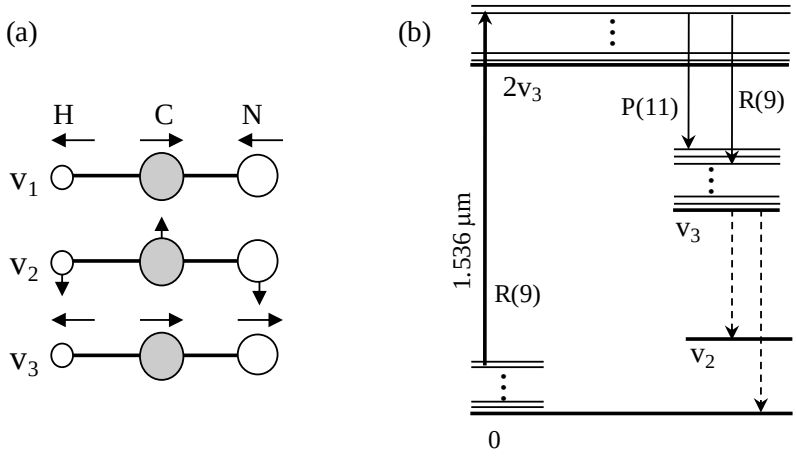

FIGURE 2. (a) Normal vibrational modes of HCN, (b) Simplified energy level diagram. An R branch pump transition from j = 9 to j = 10 and observed laser transitions at about 3100 nm and 3170 nm are shown (solid arrows). Dashed vertical arrows indicate some other possible laser transitions that were not observed in our experiments (see text).

EXPERIMENT

To demonstrate lasing in C_2H_2 and HCN using conventional gas cell, a laser cavity as shown in Fig. 3 was used. For the C_2H_2 laser, a 80 cm gas cell filled with 2.2 torr of C_2H_2 was optically pumped at the R(7) absorption line at ~ 1.521 μm by a nanosecond OPO (~ 5 ns, bandwidth ~ 3.5 GHz). The absorbed pump energy was about 2.3 mJ. The OPO pump was focused to the center of the cell by a 2-m focal length lens producing a spot of diameter about 4 mm. The 1.4-m long cavity consisted of two 5-m concave mirrors transparent to the pump wavelength and having a reflectivity ~ 0.9 in the 3.15 μm region. The laser threshold was at about 100 μJ of absorbed pump pulse energy.

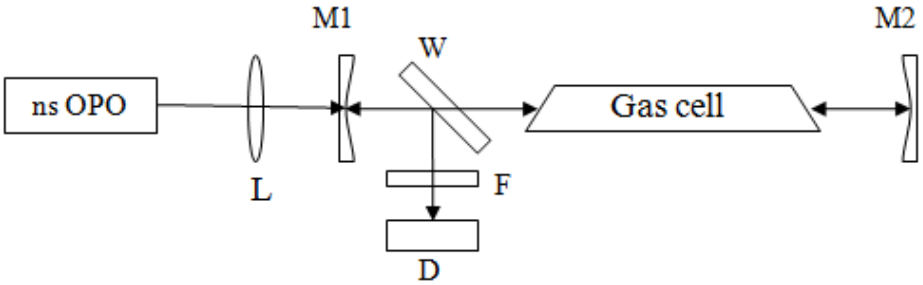

FIGURE 3. Schematic diagram of the C_2H_2 and HCN laser cavity. M1, M2: cavity mirrors, L- lens, D- fast detector. F is a filter to block the pump beam. W is a CaF_2 window to pick the laser output. For spectral measurements, the detector D was replaced by an infrared scanning spectrometer.

For the HCN laser, a 4-cm gas cell filled with 5 torr of HCN was optically pumped at the R(9) absorption line at ~ 1.536 μm by the nanosecond OPO. The cavity length

was 73 cm. The pump pulse was focused to the center of the cell using a 1-m focal length lens resulting in a spot diameter of about 2 mm. The 0.5-m radius of curvature front cavity and rear end mirrors were transparent to the pump wavelength and had a reflectivity of 0.9 in the 3 μm region. The absorbed pump energy for the 4-cm cell was about 140 μJ. The laser threshold occurred at 40 μJ of absorbed pump pulse energy.

For both lasers, the laser output was detected from the reflection off a CaF_2 window inside the laser cavity (the mirror substrate was BK7 and therefore had a low transmission at the laser wavelength). A fast HgCdTe detector was employed to record the temporal profile of the laser pulses. Spectra were recorded using a near infrared (NIR) scanning spectrometer.

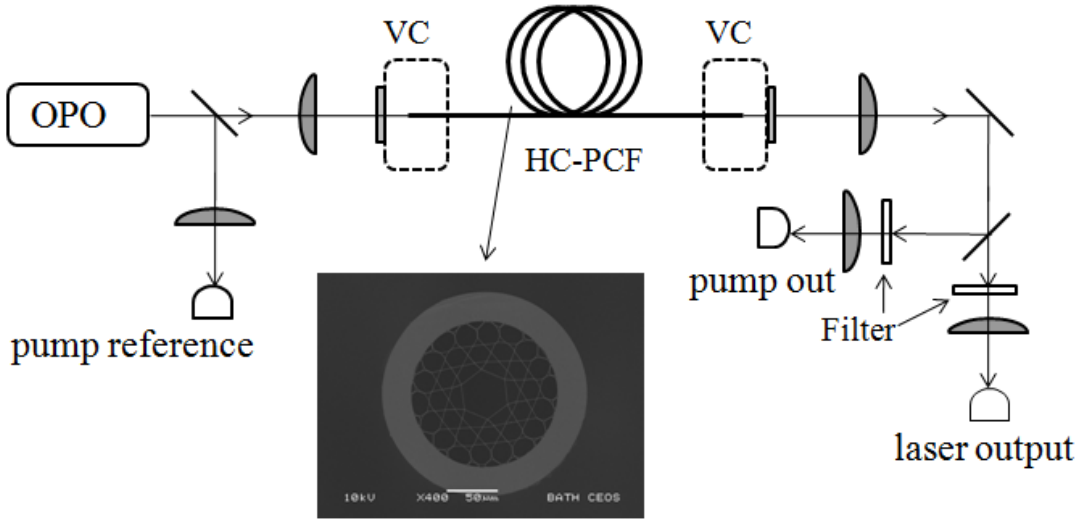

FIGURE 4. Schematic of optically pumped C_2H_2 filled hollow core fiber laser. HC-PCF: Kagome structured hollow core photonic crystal fiber, VC- vacuum chamber filled with C_2H_2. The bottom picture shows cross-section of the fiber.

The experimental layout for the optically pumped gas filled hollow core fiber laser is shown in Fig 4. Both ends of a 1.65-m Kagome structured hollow core fiber with a core diameter of ~ 40 μm were terminated in vacuum chambers, which were filled with a few torr of C_2H_2. The cross-section of the fiber is shown in Fig. 4. The measured transmission loss for the fiber was ~ 0.75 dB/m at the pump wavelength and ~20 dB/m at the lasing wavelengths. The OPO was tuned to resonance with the $v_1 + v_3$ (R7) transition of C_2H_2 at ~ 1.521 μm and was coupled to the fiber using appropriate optics. The C_2H_2 pressure was varied in the range 0.5 to 20 torr and the laser output was recorded using a fast detector for input coupled pulse energies in the range ~ 10 nJ to 2 μJ. Suitable filters were used to separate laser emission from pump at the output. The laser spectrum was recorded using a NIR scanning spectrometer.

RESULTS, INTERPRETATION AND DISCUSSION

The observed spectrum of the C_2H_2 laser from the conventional cavity is shown in Fig. 5(a), an example temporal laser profile is depicted in Fig. 5(b). The laser emission

shows two peaks separated by ~40 nm centered about 3140 nm. According to the observed laser wavelengths the two spectral components could arise from the R(7) and P(9) transitions from the terminal v_1+v_3 to the v_1 state as indicated in Fig. 2(a). The two peaks do not represent different vibration-rotation transitions from the neighboring rotational states of the terminating pump level to the same lower vibrational level; their separation would only be ~ 9 nm, estimated using the known value [16] of the rotational constant for the v_1+v_3 state. There is also the possibility that the transitions could arise from a vibrational state about 80 cm^{-1} below the upper pump level because of fast vibrational relaxation [18]. It is instructive to note the absence of any emission signature from the lower laser state v_1 to the vibrational ground state, which would be at about 3 μm. This transition is dipole forbidden [19].

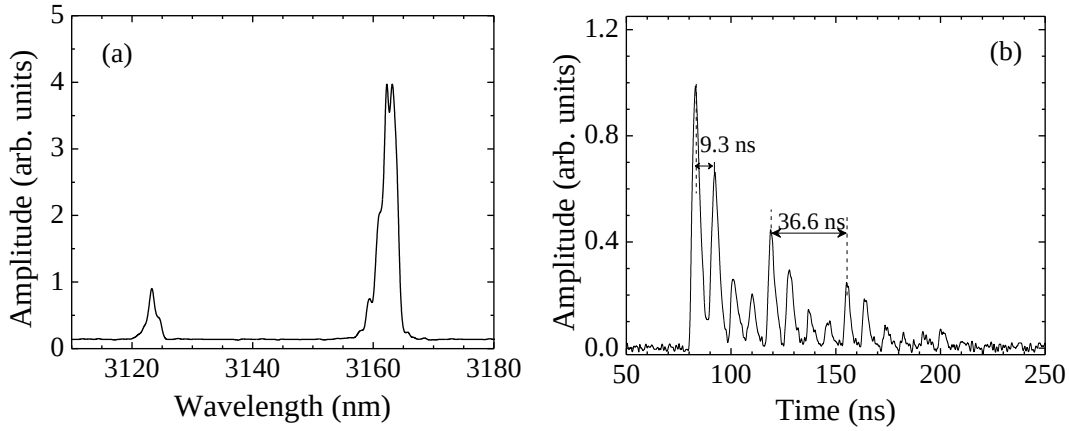

FIGURE 5. (a) Spectrum and, b) temporal profile of the C_2H_2 laser with conventional cavity pumped with 5-ns pulses at 1.521 μm. The origin of time axis corresponds to an arbitrary trigger.

The exact temporal profile of the laser output fluctuated somewhat from shot to shot and was slightly dependent on the cavity alignment. It reflects a superposition of longitudinal and transverse modes and showed the typical mode beating frequencies. The fast modulation can be attributed to longitudinal mode beating. The measured period of 9.3 ns agrees well with the beat frequency of 109 MHz obtained from our cavity geometry. The slower modulation with a period of 36.6 ns is due to transverse mode beating and is in good agreement with the expected beat frequency of ~ 26 MHz from our C_2H_2 cavity.

Figure 6 shows the spectral and temporal profile of the HCN laser. The spectrum in Fig. 6(a) shows a main peak at ~ 3165 nm. The peak likely corresponds to the P(11) transition originating from the initially populated level j = 10 of the $2v_3$ vibrational state to the v_3 state. The observed structure in the short-wavelength tail of the peak could arise from P line emission originating at adjacent rotational states (j = 8 and j = 9) because of the short (~ 5 ns) rotational relaxation time [20].

The exact relaxation pathway from the lower laser level to the ground state and relevant time constants are not completely known. There is a possibility for another laser transition between vibrational levels v_3 and v_2 producing radiation at about 4 μm [21]. There is also another potential laser transition from level v_3 to the ground state, which

would emit at about 3 microns [21]. None of these lasing lines were observed. Likely reasons are insufficient pump energy and inadequate bandwidth of the cavity mirrors.

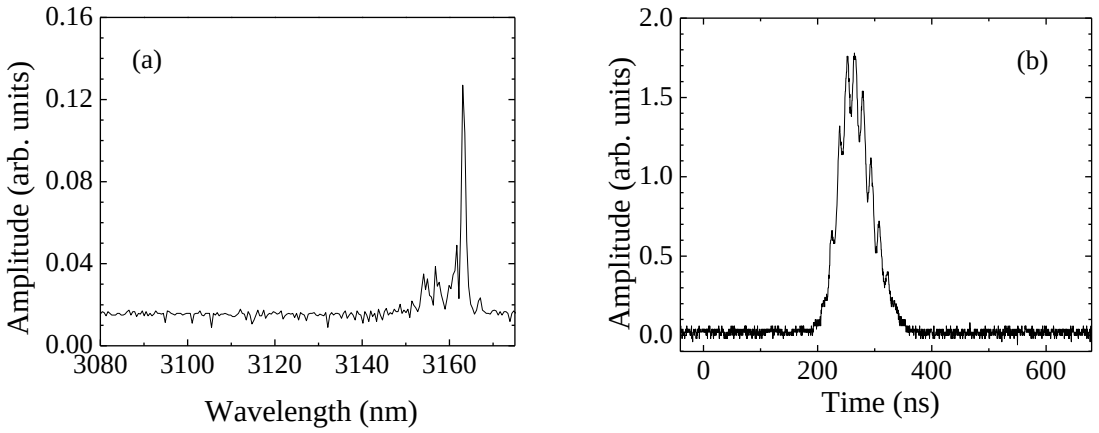

FIGURE 6. (a) Spectrum, and (b) temporal profile of an HCN laser pumped with 5-ns pulses at 1.536 μm in a conventional laser cavity configuration.

The temporal profile of the HCN laser output is distinctly different from the C_2H_2 laser output. Owing to the shorter gas cell of the former, more cavity roundtrips are needed before the pulse peak. Thus mode competition for the available gain is more pronounced and almost entirely suppresses higher-order modes. Therefore only small modulation (mode beating) in the HCN laser output is visible. The beat frequencies of about 240 MHz and 71 MHz, respectively are what is expected for the longitudinal and transverse mode spacing from the cavity parameters.

No attempt was made to optimize the laser output by finding optimum gas pressures and cavity configurations. The observed laser efficiencies in terms of absorbed pump energies were of the order of 10% for the C_2H_2 and HCN laser.

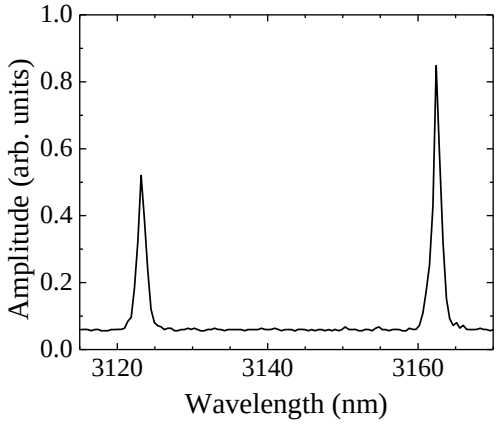

FIGURE 7. Spectrum of the C_2H_2 filled HC-PCF laser. The C_2H_2 pressure was 7 torr.

Figure 7 shows the spectral profile of the acetylene filled HC-PCF laser for a pressure of 7 torr. The lasing threshold, defined as the minimum pump pulse energy

coupled into the fiber necessary to observe mid-IR laser output, is about 200 nJ and varies with pressure. The observed laser lines were the same as those seen by conventional gas cell and cavity.

Figure 8(a) shows the HC-PCF laser output as a function of pump pulse energy for two pressures, 2 and 7 torr of acetylene. This curve indicates the onset of saturation as the increasing pump pulse energy starts to saturate the absorption transition. At lower pressures, saturation is more pronounced.

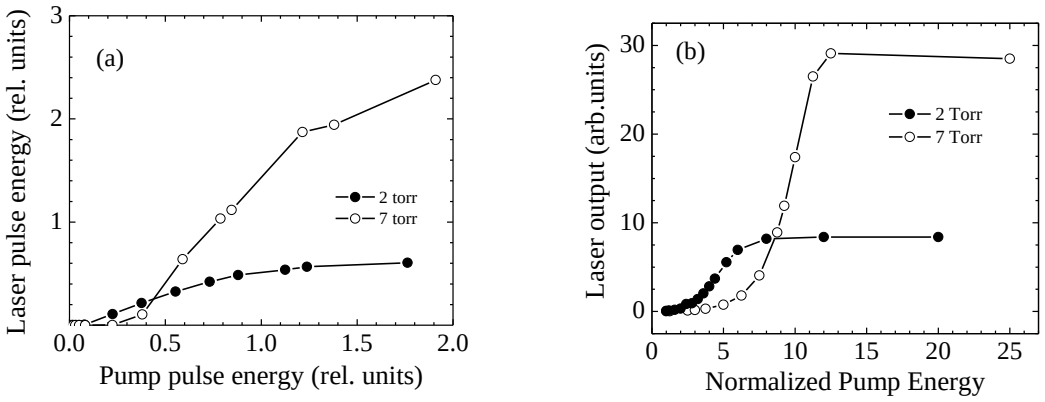

FIGURE 8. (a) Experimentally observed laser pulse energy as a function of pump energy, and (b) simulated laser output using a saturable absorber/amplifier model.

We have we used a simple model to qualitatively predict the trends observed in the experiment. A Gaussian pump pulse in resonance with the gas was sent through the fiber, which creates a population inversion. The laser pulse develops from spontaneous emission. In this model, both pump and probe (laser) saturate the respective transitions. The linear fiber losses were taken into account. Figure 8(b) shows the laser output as a function of input energy as predicted by the model. The results are in qualitative agreement with the experiment. The model also can be used to predict the optimum fiber length for maximum laser output.

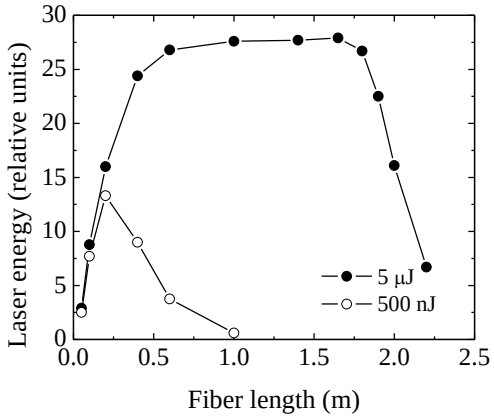

FIGURE 9. Laser energy as a function of fiber length as predicted by the model. The C_2H_2 pressure was 7 torr.

Figure 9 shows as an example the calculated laser energy as a function of fiber length for two input energies, 500 nJ and 5 μJ, for an acetylene pressure of 7 torr. As is evident, there is an optimum fiber length for a given input energy and pressure. This optimum arises from the interplay of pump depletion along the fiber and the relatively large linear losses at the laser wavelength in the current system.

The slope efficiency of the laser, defined as the change in output energy divided by the change in pump energy coupled into the fiber, is a few percent. In this initial demonstration, no attempt was made to optimize the laser output by finding the optimal pressure, fiber length and other parameters. Optimization of these parameters would result in higher slope efficiency. A different Kagome design with lower losses at the laser wavelength would also increase the efficiency.

In summary, we have demonstrated lasing of C_2H_2 and HCN near 3 μm when pumped in a conventional gas cell/cavity with a nanosecond OPO in the 1.5 μm region. We have also demonstrated for the first time, mid-IR (~ 3 μm) lasing from a C_2H_2 filled HC-PCF based on population inversion when pumped at 1.5 μm. With suitable fiber bandwidths, the gas filled HC-PCF is likely to give similar results with many other molecular gases, including HCN.

ACKNOWLEDGMENTS

The authors acknowledge support from Air Force Office of Scientific Research (FA9550-08-1-0344), Army Research Office (W911NF-08-C-0106 and W911NF-08-1-0332), National Science Foundation (PHY-0722622), Joint Technology Office (W911NF-05-1-0507), Engineering and Physical Sciences Research Council, and Precision Photonics Corp. We are grateful to Michael Heaven (Emory University) for sharing preliminary C_2H_2 spectroscopic data with us.

REFERENCES

1. Gourevitch, G. Venus, V. Smirnov, D.A. Hostutler, and L. Glebov, *Opt. Lett.* **33**, 702-704 (2008).
2. J.F. Sell, W.Miller, D.Wright, B.V. Zhdanov, and R.J. Knize, *Appl. Phys. Lett.* **94**, 051115-1 – 051115-3 (2009).
3. N. Jovanovic, M. Aslund, A. Fuerbach, S. D. Jackson, G. D. Marshall, and M. J. Withford, *Opt. Lett.* **32**, 2804-2806 (2007).
4. L. S. Meng, B. Nizamov, P. Madasamy, J. K. Brasseur, T. Henshaw, and D. K. Neumann, *Opt. Express* **14**, 10469-10474 (2006).
5. T. Ehrenreich, B. Zhdanov, T. Takekoshi, S.P. Phipps, and R.J. Knize, *Electron. Lett.* **41**, 415-416 (2005).
6. B.V. Zhdanov, M.K. Shaffer, and R.J. Knize, *Opt. Express* **17**, 14767-14770 (2009).
7. A.V.V.Nampoothiri, A.Ratanavis, N.Cambell, and W.Rudolph, *Opt. Express* **18**, 1946-1951 (2010).
8. Yoonchan Jeong, Member, IEEE, Seongwoo Yoo, Christophe A. Codemard, Johan Nilsson, Jayanta K. Sahu, David N. Payne, R. Horley, P. W. Turner, Louise Hickey, Andrew Harker, Mike Lovelady, and Andy Piper, *IEEE Journal of Sel. Topics In Quantum Electron*. **13**, 573-579 (2007).
9. Jens Limpert, Fabian R¨oser, Sandro Klingebiel, Thomas Schreiber, Christian Wirth, Thomas Peschel, Ramona Eberhardt, and Andreas Tunnermann, *IEEE Journal of Sel. Topics In Quantum Electron*. **13**, 537-545 (2007).
10. Rajesh Thapa, Kevin Knabe, Mohammed Faheem, Ahmer Naweed, Oliver L. Weaver, and Kristan L. Corwin, *Opt. Lett.* **31**, 2489-2491 (2006).

11. F. Benabid, J. C. Knight, G. Antonopoulos, and P. St. J. Russell, *Science* **298**, 399-402 (2002).
12. F. Couny, F. Benabid, and P. S. Light, *Phys. Rev. Lett.* **99**, 143903-1—143903-4 (2007).
13. P. J. Roberts, F. Couny, H. Sabert, B. J. Mangan, D. P. Williams, L. Farr, M. W. Mason, A. Tomlinson, T. A. Birks, J. C. Knight, and P. St.J. Russell, *Opt. Express* **13**, 236-244 (2005).
14. F. Couny, F. Benabid, and P. S. Light, *Optics Letters* **31**, 3574-3576 (2006).
15. A. Ratanavis, N. Campbell, and W.Rudolph, *Opt. Commun.* **283** 1075-1080 (2009).
16. M.Herman, A.Campargue, M. I. El Idrissi, and J. Vander Auwera, *J. Phys. Chem. Ref. Data* **32**, 921-1361 (2003).
17. W. C. Swann and S.L. Gilbert, *J. Opt. Soc. Am. B* **22**, 1749-1756 (2005).
18. M.C.Heaven (private communication).
19. G. Herzberg, *Infrared and Raman Spectra,* D. Van Nostrand Company:New York, 1945.
20. J.Wu, R.Huang, M.Gong, A.Saury, and E.Carrasquillo, *J. Chem. Phys.* **99**, 6474-6482 (1993).
21. A.M. Smith, S. L. Coy, and W. Klemperer, *J. Mol. Spec.* **134**,134-153 (1989).

Laser emission from a gas (acetylene) filled hollow fiber

A.V.V. Nampoothiri[1], A. M. Jones[2] , A. Ratanavis[1], R. Kadel[1], N. Wheeler[3], F. Couny[3], F. Benabid[3], B. R. Washburn[2], K. L. Corwin[2], and W. Rudolph[1]

[1]*Department of Physics and Astronomy, University of New Mexico, Albuquerque, NM-87131, USA*

[2]*Department of Physics, Kansas State University, Manhattan, KS 66506, USA*

[3]*Centre for Photonics and Photonic Materials, Department of Physics, University of Bath, Claverton Down, Bath BA2 7AY, United Kingdom*

We demonstrate what we believe is the first hollow fiber gas laser based on population inversion. A single-cell kagome fiber with a core diameter of about 20 μm was filled with a few torr of acetylene ($^{12}C_2H_2$). Acetylene has absorption transitions in the telecommunication C band region and recently lasing was observed near 3 μm from a gas cell when optically pumped. This kagome fiber exhibits strong guiding in the near IR pump region (loss ~0.75 dB/m) and weak guiding behavior at about 3 μm (~20 dB/m), as calculations suggest. Pumping the gas filled fiber (1.65 m) with μJ pulses from a 5-ns OPO resulted in the emission of two laser lines at 3.12 μm and 3.16 μm. These lines correspond to the R(7) and P(9) transitions originating from the initially populated rotational state of the (10100) vibrational level and terminating at the (10000) vibrational state of acetylene. In this configuration both the pump and laser pulses saturate the respective transitions. The laser combines the advantages of fiber lasers, such as the confinement of pump and laser light over long interaction lengths in a compact configuration, with those of gas lasers: high damage thresholds, a wide variety of possible emission wavelengths, and the potential for coherent emission from mutually incoherent pump sources. While this first demonstration used a pulsed pump, the gas filled fiber laser is particularly attractive for pumping with CW laser sources.

Presented at Photonics West 2011 as a postdeadline paper.